Supporting Information

Chiral Plasmonic Liquid Crystal Gold Nanoparticles: Self-Assembly into Circular Dichroism Responsive Helical Lamellar Superstructure

*Sachin A. Bhat, D. S. Shankar Rao, S. Krishna Prasad and Channabasaveshwar V. Yelamaggad**

Centre for Nano and Soft Matter Sciences (CeNS)
P. B. No. 1329, Prof. U. R. Rao Road, Jalahalli, Bengaluru 560012, India
*Corresponding author. E-mail: yelamaggad@cens.res.in.
Homepage: http://www.cens.res.in/index.php/faculty/yelamaggad/profile

CONTENTS

Synthesis and characterization of cholesteryl ω-bromoalkanoates (**1a-c**):

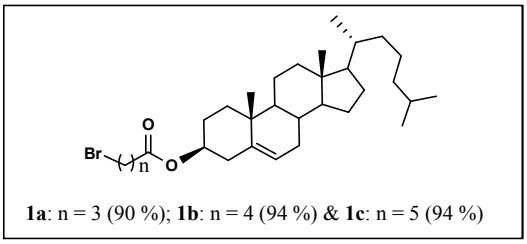

1a: n = 3 (90 %); **1b**: n = 4 (94 %) & **1c**: n = 5 (94 %)

General procedure: Oxallyl chloride (12 ml) was added to ω-bromoalkanoic acid (1 equiv.) and stirred at rt for 4 h under nitrogen atmosphere. The excess of oxalyl chloride was distilled out under reduced pressure and the ω-bromoalkanoyl chloride obtained was thoroughly dried under *vacuo* and was added dropwise to a solution of cholesterol (1 equiv.) in pyridine (6 ml) and dry THF (50 ml) at 0^{o} C. The reaction mixture was slowly allowed to attain rt and stirred for 12 h. The reaction mixture was filtered on celite bed. Evaporation of the solvent from the filtrate furnished a pale yellow mass which was dissolved in a mixture of CH_2Cl_2 and Et_2O (20:80). The organic layer was thoroughly washed with water, brine and dried over anhyd. Na_2SO_4. The crude mass obtained upon evaporation of the solvent was purified by column chromatography using neutral alumina. Elution with a mixture of 30% CH_2Cl_2-hexanes afforded the pure product.

1a: Cholesteryl 4-bromobutanoate

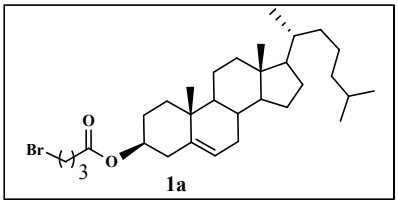

1a

R_f = 0.33 in 30% CH_2Cl_2-hexanes; a white solid; yield: 90 %; m.p.: 87-88 °C; IR (KBr Pellet): ν_{max} in cm^{-1}: 2950, 2890, 1739, 1567; ^{1}H NMR (400MHz, $CDCl_3$): δ 5.37 (brd, J = 3.8 Hz, 1H, 1 × olefinic), 4.65 (m, 1H, 1 × CHOCO), 3.74 (t, J = 6.5 Hz, 2H, 1 × CH_2Br), 2.48 (m, 4H, 2 × allylic CH_2), 2.03-1.05 (m, 28H, 11 × CH_2, 6 × CH), 1.01 (s, 3H, 1 × CH_3), 0.92 (d, J = 6.4 Hz, 3H, 1 × CH_3), 0.87 (d, J = 1.4 Hz, 3H, 1 × CH_3), 0.85 (d, J = 1.4 Hz, 3H, 1 × CH_3) and 0.67 (s, 3H, 1 × CH_3); Anal. calcd for $C_{31}H_{51}BrO_2$: C, 69.50; H, 9.59. Found: C, 70.01; H, 9.22.

1b: Cholesteryl 5-bromopentanoate

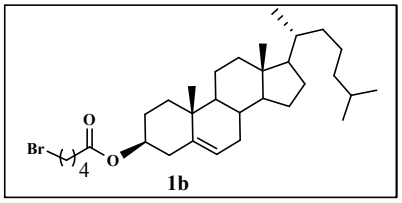

1b

R_f = 0.30 in 30% CH_2Cl_2-hexanes; a white solid; yield: 94 %; m.p.: 101-102 °C; IR (KBr Pellet): ν_{max} in cm^{-1}: 2949, 2860, 1725, 1563; ^1H NMR (400MHz, $CDCl_3$): δ 5.38 (brd, J = 3.8 Hz, 1H, 1 × olefinic), 4.62 (m, 1H, 1 × CHOCO), 3.43 (t, J = 6.5 Hz, 2H, 1 × CH_2Br), 2.33 (m, 4H, 2 × allylic CH_2), 2.03-1.01 (m, 30H, 12 × CH_2, 6 × CH), 1.01 (s, 3H, 1 × CH_3), 0.92 (d, J = 6.5 Hz, 3H, 1 × CH_3), 0.87 (d, J = 1.6 Hz, 3H, 1 × CH_3), 0.86 (d, J = 1.8 Hz, 3H, 1 × CH_3) and 0.68 (s, 3H, 1 × CH_3); Anal. Calcd. for $C_{32}H_{53}BrO_2$: C, 69.91; H, 9.71. Found: C, 69.86; H, 9.75.

1c: Cholesteryl 6-bromohexanoate

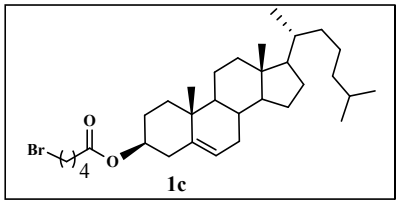

1c

R_f= 0.25 in 30% CH_2Cl_2-hexanes; a white solid; yield: 94 %; m.p.: 100.57 °C; IR (KBr Pellet): ν_{max} in cm^{-1}: 2944, 2864, 1730, 1557; ^1H NMR (400MHz, $CDCl_3$): δ 5.38 (brd, J = 3.8 Hz, 1H, 1 × olefinic), 4.63 (m, 1H, 1 × CHOCO), 3.42 (t, J = 6.8 Hz, 2H, 1 × CH_2Br), 2.31 (m, 4H, 2 × allylic CH_2), 2.03-1.04 (m, 32H, 13 × CH_2, 6 × CH), 1.01 (s, 3H, 1 × CH_3), 0.92 (d, J = 6.5 Hz, 3H, 1 × CH_3), 0.87 (d, J = 1.8 Hz, 3H, 1 × CH_3), 0.85 (d, J = 1.8 Hz, 3H, 1 × CH_3) and 0.67 (s, 3H, 1 × CH_3); Anal. calcd for $C_{33}H_{55}BrO_2$: C, 70.30; H, 9.56. Found: C, 70.66; H, 9.56.

Synthesis and characterization of cholesteryl ω-(4-nitrophenoxy)alkanoates (**2a-c**)

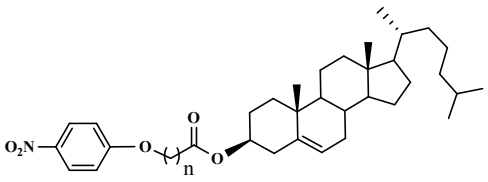

2a: n = 3; **2b**: n = 4 & **2c**: n = 5

A mixture of cholesteryl ω-bromoalkanoates (**1a-c**) (1 equiv.), 4-nitrophenol (1.2 equiv.) and anhyd. K_2CO_3 (1.5 equiv.) in dry DMF (20 ml) was degassed and stirred at 85 °C for 12 h under nitrogen atmosphere. The hot reaction mixture was filtered through celite bed

and the filtrate was concentrated and poured into water. The off-white solid separated was collected by filtration. It was purified by recrystallization from CH_2Cl_2-ethanol (1:9) to yield yellow solid.

2a: Cholesteryl 4-(4-nitrophenoxy)butanoate

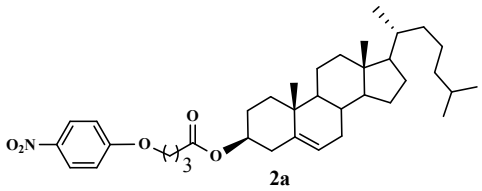

2a

R_f = 0.43 in 30% CH_2Cl_2-hexanes; a white solid; yield: 82 %; Phase sequence: Cr 133.59 (34.49) I; I 130.32 (1.07) N* 117.15 (0.89) TGB-SmA 88.96 (1.94) Cr; IR (KBr Pellet):ν_{max} in cm^{-1}: 2946, 2867, 1733, 1592, 1510, 1378, 1338, 1178, 1111; ^{1}H NMR (400MHz, $CDCl_3$): δ 8.20 (d, J = 6.8 Hz, 2H,Ar), 6.96 (d, J = 7.2Hz, 2H,Ar), 5.38 (brd, *J* = 3.6 Hz, 1H, 1 × olefinic),4.68-4.60 (m, 1H, 1 × CHOCO),4.13(t, 2H, 6.4Hz, 1 × OCH_2) 2.31 (m, 4H, 2 × allylic CH_2) and 2.16-0.68 (m, 43H, 6×CH, 11×CH_2, 5×CH_3);Anal. calcd for $C_{37}H_{55}NO_5$: C, 74.83; H, 9.34, N, 2.36. Found: C, 74.25; H, 8.97, N.2.72.

2b: Cholesteryl 5-(4-nitrophenoxy)pentanoate

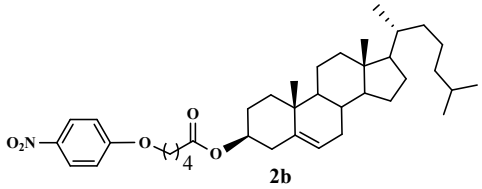

2b

R_f = 0.44 in 30% CH_2Cl_2-hexanes; a white solid; yield: 83 %; Phase sequence: Cr 106.88 (0.735) N* 124.96 (1.009) I ; I 123.92 (1.14) N* 113.2 TGB-SmA 105.95 (0.85) Cr;IR (KBr Pellet): ν_{max} in cm^{-1}: 2946, 2867, 1733, 1592, 1510, 1386, 1338,1178, 1110; ^{1}H NMR (400MHz, $CDCl_3$): δ 8.20 (d, *J* = 6.8 Hz, 2H,Ar), 6.95 (d, *J* = 7.2Hz, 2H,Ar), 5.37 (brd, *J* = 3.6 Hz, 1H, 1 × olefinic),4.66-4.58 (m, 1H, 1 × CHOCO), 4.09 (t, 6.0 Hz, 2H, 1 × OCH_2), 2.39-2.30 (m, 4H, 2 × allylic CH_2) and 2.03-0.68 (m, 45H, 6×CH, 12×CH_2, 5×CH_3); Anal. calcd for $C_{38}H_{57}NO_5$: C, 75.08; H, 9.45, N, 2.30. Found: C, 75.27; H, 9.547, N, 3.07

2c: Cholesteryl 6-(4-nitrophenoxy)hexanoate

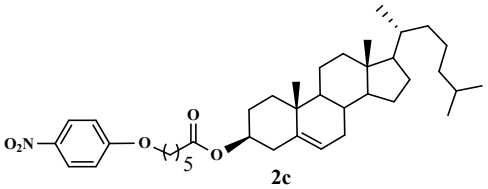

2c

R_f = 0.44 in 30% CH_2Cl_2-hexanes; a white solid; yield: 85 %; Phase sequence: Cr 136.30 (30.70) I; I 124.39 (1.11) N* 102.38 (18.25) Cr; IR (KBr Pellet): ν_{max} in cm^{-1}: 2946, 2867, 1732, 1592, 1511, 1386, 1338, 1178, 1118; ^1H NMR (400MHz, $CDCl_3$): δ 8.20 (d, J = 7.2 Hz, 2H, Ar), 6.94 (d, J = 6.8 Hz, 2H, Ar), 5.37 (brd, J = 4 Hz, 1H, 1 × olefinic), 4.66-4.58 (m, 1H, 1 × CHOCO), 4.07 (t, J = 6.4 Hz, 2H, 1 × OCH_2), 2.34-2.30 (m, 4H, 2 × allylic CH_2) and 2.00-0.68 (m, 47H, 6×CH, 13×CH_2, 5×CH_3); Anal. calcd for $C_{39}H_{59}NO_5$: C, 75.32; H, 9.56, N, 2.25. Found: C, 76.06; H, 9.29, N, 3.09.

Synthesis and characterization of cholesteryl ω-(4-aminophenoxy)alkanoates (**LCL-4, 5** & **6**):

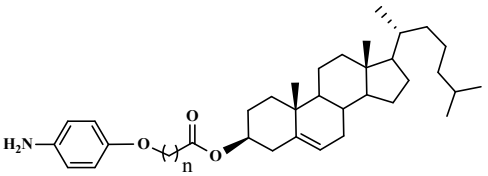

LCL-4: n = 3; **LCL-5**: n = 4 & **LCL-6**: n = 5

Cholesteryl ω-(4-nitrophenoxy)alkanoates (2g, 1 equiv.) was dissolved in dry THF and 10% Pd-C (10% weight of the nitro compound) was added. The reaction mixture was degassed and stirred under H_2 gas (1 atmospheric pressure) for 10 h at room temperature. The reaction mixture was filtered over celite bed, concentrated and the solid obtained was recrystallized from hexanes to afford an off-white solid.

LCL-4: Cholesteryl 4-(4-aminophenoxy)butanoate

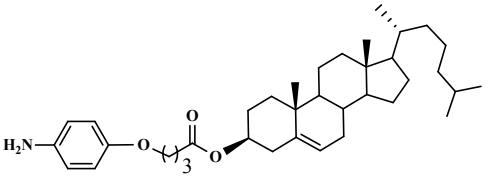

LCL-4

R_f = 0.49 in 50% CH_2Cl_2-hexanes; a white solid; yield: 87 %; IR (KBr Pellet): ν_{max} in cm^{-1}: 3376, 2937, 2868, 1726, 1179, 1103; ^1H NMR (400 MHz, $CDCl_3$): δ 6.73 (d, J = 6.8 Hz, 2H, Ar), 6.64 (d, J = 6.8 Hz, 2H, Ar), 5.37 (brd, J = 3.6 Hz, 1H, 1 × olefinic), 4.63 - 4.60 (m, 1H, 1

× CHOCO), 3.91 (t, *J* = 6 Hz, 2H, 1 × OCH_2), 3.42 (brs, 2H, 1× NH_2), 2.35 - 2.30 (m, 4H, 2 × allylic CH_2) and 1.99 - 0.68 (m, 43H, 6 × CH, 11 × CH_2, 5 × CH_3); ^{13}C NMR (100 MHz, $CDCl_3$): 172.82, 152.10, 140.10, 139.74, 122.72, 116.46, 115.75, 67.54, 56.75, 56.19, 50.08, 39.59, 36.25, 35.88, 31.92, 31.30, 28.32, 28.10, 24.94, 23.90, 22.92, 22.65, 19.40, 18.79 and 11.93; Anal. calcd for $C_{37}H_{57}NO_3$: C, 78.81; H, 10.19, N, 2.48. Found: C, 78.31; H, 10.25, N,2.72.

LCL-5: Cholesteryl 5-(4-aminophenoxy)pentanoate

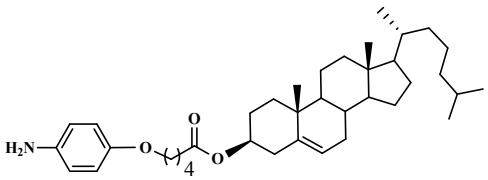

LCL-5

Rf = 0.49 in 50% CH_2Cl_2-hexanes; a white solid; yield: 92 %; IR (KBr Pellet): ν_{max} in cm^{-1}: 3376, 2938, 2869, 1726, 1179, 1103; ^1H NMR (400 MHz, $CDCl_3$): δ 6.74 (d, *J* = 6.4 Hz, 2H, Ar), 6.65 (d, *J* = 6.8 Hz, 2H, Ar), 5.37 (brd, *J* = 3.6 Hz, 1H, 1 × olefinic), 4.66 - 4.57 (m, 1H, 1 × CHOCO), 3.89 (t, J = 6.4 Hz, 2H, 1 × OCH_2), 3.40 (brs, 2H, 1× NH_2), 2.32 - 2.28 (m, 4H, 2 × allylic CH_2) and 1.99 - 0.68 (m, 45H, 6 × CH, 12 × CH_2, 5 × CH_3); ^{13}C NMR (100 MHz, $CDCl_3$): 173.34, 152.29, 139.974, 139.77, 122.69, 116.48, 115.70, 68.39, 56.76, 56.49, 56.32, 54.28, 50.08, 42.38, 39.59, 35.88, 35.54, 29.17, 28.10, 25.73, 22.91, 22.65, 19.41, 18.79, 18.74, 12.31, 12.15 and 11.94; Anal. calcd for $C_{38}H_{59}NO_3$: C, 78.98; H, 10.29, N, 2.42. Found: C, 79.30, H, 10.82, N,2.36.

LCL-6: Cholesteryl 6-(4-aminophenoxy)hexanoate

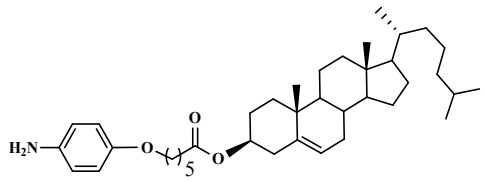

LCL-6

R_f = 0.50 in 50% CH_2Cl_2-hexanes; a white solid; yield: 90 %; IR (KBr Pellet): ν_{max} in cm^{-1}: 3374, 2940, 2869, 1726, 1179, 1102; ^1H NMR (400 MHz, $CDCl_3$): δ 6.66 (d, *J* = 6.4 Hz, 2H, Ar), 6.57 (d, J = 6.4 Hz, 2H, Ar), 5.30 (brd, *J* = 4.0 Hz, 1H, 1 × olefinic), 4.58 - 4.52 (m, 1H, 1 × CHOCO), 3.85 (t, J = 6.4 Hz, 2H, 1 × OCH_2), 3.39 (brs, 2H, 1× NH_2), 2.28 - 2.23 (m, 4H, 2 × allylic CH_2) and 1.92 - 0.61 (m, 47H, 6×CH, 13 × CH_2, 5 × CH_3); ^{13}C NMR (100 MHz, $CDCl_3$): 173.19, 152.29, 139.95, 139.77, 122.70, 116.48, 115.70, 68.39, 56.76, 56.19, 50.08,

39.59, 35.88, 31.92, 29.17, 28.32, 28.10, 25.73, 24.91, 23.90, 22.91,. 22.65, 19.41, 18.79, and 11.94; Anal. calcd for $C_{39}H_{61}NO_3$: C, 78.14; H, 10.39, N, 2.37. Found: C, 79.41, H, 10.63, N, 2.38.

Preparation and characterization of liquid crystal-gold nanoparticles (**LC-GNP-4, 5** & **6**):

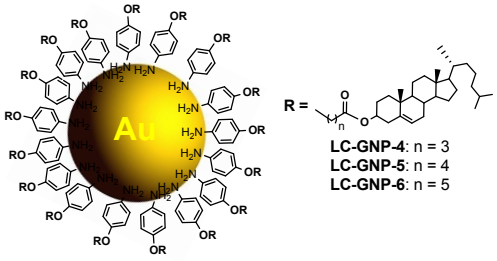

Solution method: To dichloromethane (DCM) (~ 15 ml) placed in a sample bottle, was added an aqueous solution of hydrogen tetrachloroaurate(III) ($HAuCl_4.3H_2O$) (10.2 mg, 30 mmol) dissolved in deionized water (~ 8 ml) at room temperature (RT); the top aqueous phase of the liquid bilayer appears pale-yellow due to the presence of Au(III) ions. To the resultant liquid bilayer was added a solution of tetraoctylammonium bromide (TOAB) (27.3 mg, 50 mmol) dissolved a minimum quantity DCM and the mixture was hand-swirled vigorously; here, the organic phase (DCM) gains intense yellow colour owing to the presence of Au(III) ions. To a well-settled liquid bilayer, a solution of chosen liquid crystal ligand (**LCL-4**, Qty. 101.3 mg; or **LCL-5**, Qty. 104.2 mg or **LCL-6**, Qty. 106.5 mg**)** (180 mmol, 6 equivalent) dissolved in minimum quantity of DCM was slowly added drop-wise while hand-swirling; after completion of addition the mixture was continued to hand-swirl for a while; the colour of organic layer appears to be deep-red implying the instant interaction between the LCL and GNPs resulting into the formation of **LC-GNPs**. The bilayer was allowed to settle and the organic layer separated and collected was thoroughly washed with deionized water repeatedly. The solvent was evaporated under high vacuum and the dark-purple mass obtained was washed with a hot mixture of ethanol-DCM (9:1) thoroughly. This process ensures the removal of unused LCL as well as TOAB (TLC monitored; $KMnO_4$ stain). The sample obtained after centrifugation was further purified by dissolving in minimum amount of DCM and reprecipitated by adding ethanol in large excess. After centrifugation, the pure **LC-GNPs** obtained were dried in vacuum and stored in sample vials under normal atmospheric conditions.

Role of TOAB: Tetraoctylammonium bromide (TOAB), being ambipolar system (comprising both hydrophobic and hydrophilic segments) acts as phase transfer catalyst. Thus, it enables the migration of gold (III) ions from the aqueous solution to organic solvent where it reversibly

binds to gold (III) chloride and moves it towards organic layer. The preparation of organic gold solution is absolutely necessary because the ligand, which acts as the reducing agent and capping organic molecules, is soluble in organic solvent only.

Drop-casting method: On a clean glass plate, a solution of hydrogen tetrachloroaurate(III) ($HAuCl_4.3H_2O$) (0.6 mg, 1.5 mmol) and TOAB (1.4 mg, 2.5 mmol) in DCM (~ 0.4 ml) was drop-casted at room temperature (RT) and the DCM was allowed to evaporate naturally to obtain a pale-yellow thin-film of Au(III) ions. Over this film a solution of mesogen (**LCL-4**, Qty. 5.05 mg; or **LCL-5**, Qty. 5.21 mg or **LCL-6**, Qty. 5.32 mg**)** (9 mmol, 6 equivalent) in DCM (~ 0.3 ml) was dropped at once. The colour of the glass substrate instantly changes to deep-reddish/pinkish due to the generation of **LC-GNPs**. The DCM was allowed to evaporate and the dark-pinkish film formed on the glass substrate was washed with deionized water repeatedly to ensure the removal of unused Au(III) ions. Subsequently, the film was washed thoroughly with a mixture of ethanol-DCM (9:1) to remove the leftover LCLs and TOAB. The film was air-dried and covered with watch glass. The characteristics of **LC-GNPs** adhering to glass plate were found matching with those of NPs prepared by solution method. In order to obtain frozen LC film, the above mentioned film of as-prepared sample was heated to ~ 235 ^oC (isotropic temperature) and cooled gradually at a rate of 10 ^oC / min.

LC-GNP-4: GNPs coated with cholesteryl 4-(4-aminophenoxy)butanoate

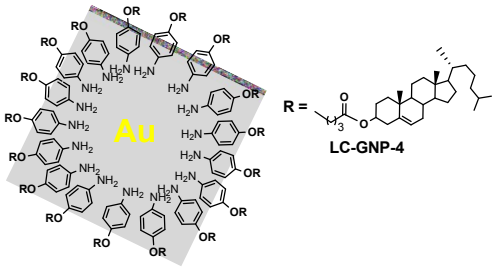

Deeply dark-red solid; yield: 35 %; IR (KBr Pellet): ν_{max} in cm^{-1}: 3356, 2950, 2864, 1731, 1674, 1511, 1470, 1376, 1250, 1172, 1056, 825; ^1H NMR (400 MHz, $CDCl_3$): δ 7.25 (d, J = 12Hz, 2H, Ar), 6.83 (d, J = 8Hz, 2H, Ar), 5.37 (brs, 1H, 1 × olefinic), 4.63-4.60 (m, 1H, 1 × CHOCO), 3.95 (m, 2H, 1× OCH_2) and 2.32-0.68 (m, 43H, 6 × CH, 11 × CH_2, 5 × CH_3); ^{13}C NMR (100 MHz, $CDCl_3$): 173.22, 152.28, 139.93, 139.76, 122.71, 116.49, 115.69, 73.87, 68.37, 56.75, 56.18, 50.07, 42.38, 39.59, 36.67, 35.88, 29.18, 28.11, 25.73, 22.93, 22.66, 19.42, 18.80 and 11.94. Elemental analysis: Weight % in **LC-GNP-4**; C: 78.43, H: 10.31 & N: 2.40; Weight % in **LCL-4**; C: 78.31, H: 10.25 & N: 2.72;

LC-GNP-5: GNPs coated with cholesteryl 5-(4-aminophenoxy)pentanoate

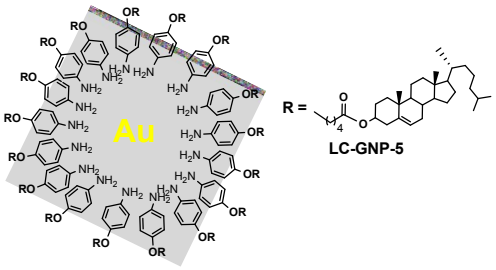

Deeply dark-red solid; yield: 32 %; IR (KBr Pellet): ν_{max} in cm^{-1}: 3356, 2950, 2864, 1731, 1674, 1511, 1470, 1179, 1376, 1250, 1172, 1056, 825; ^{1}H NMR (400 MHz, $CDCl_3$): δ 6.88 (d, *J* = 8 Hz, 2H, Ar), 6.84 (d, J = 8 Hz, 2H, Ar), 5.37 (brs, 1H, 1 × olefinic), 4.63-4.60 (m, 1H, 1 × CHOCO), 3.91 (m, 2H, 1× OCH_2) and 2.32-0.68 (m, 45H, 6 × CH, 12 × CH_2, 5 × CH_3); ^{13}C NMR (100 MHz, $CDCl_3$): 173.45, 152.52, 139.78, 121.22, 116.43, 115.75, 103.00, 68.75, 56.73, 56.19, 50.08, 42.35, 39.78, 39.54, 38.20, 37.04, 36.22, 35.80, 34.73, 31.91, 29.35, 29.19, 29.10, 28.23, 28.02, 27.85, 26.04, 25.06, 23.85, 22.81, 22.56, 21.06, 19.33, 18.73, and 11.87. Elemental analysis: Weight % in **LC-GNP-5**; C: 78.52, H: 10.66 & N: 1.98; Weight % in **LCL-5**; C: 79.30, H: 10.82 & N: 2.36.

LC-GNP-6: GNPs coated with cholesteryl 6-(4-aminophenoxy)hexanoate

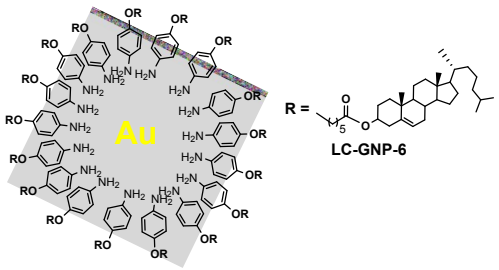

Deeply dark-red solid; yield: 28 %; IR (KBr Pellet): ν_{max} in cm^{-1}: 3345, 2946, 2867, 1731, 1673, 1512, 1469, 1512, 1469, 1381, 1240, 1170, 1030, 824; ^{1}H NMR (400 MHz, $CDCl_3$): δ 7.47 (d, *J* = 8 Hz, 2H, Ar), 6.90 (d, J = 8 Hz, 2H, Ar), 5.38 (brs, 1H, 1 × olefinic), 4.63-4.61 (m, 1H, 1 × CHOCO), 3.95 (m, 2H, 1× OCH_2) and 2.32-0.68 (m, 47H, 6×CH, 13 × CH_2, 5 × CH_3); ^{13}C NMR (100 MHz, $CDCl_3$): 172.84, 152.12, 140.03, 139.73, 122.73, 116.50, 115.73, 76.86, 76.79, 76.76, 74.07, 67.52, 56.75, 56.18, 50.07, 42.38, 39.59, 36.67, 35.88, 31.92, 28.10, 23.90, 22.92, 19.41, 18.80 and 11.94. Elemental analysis: Weight % in **LC-GNP-6**; C: 78.40, H: 10.83 & N: 2.08; Weight % in **LCL-6**; C: 79.41, H: 10.63 & N: 2.38

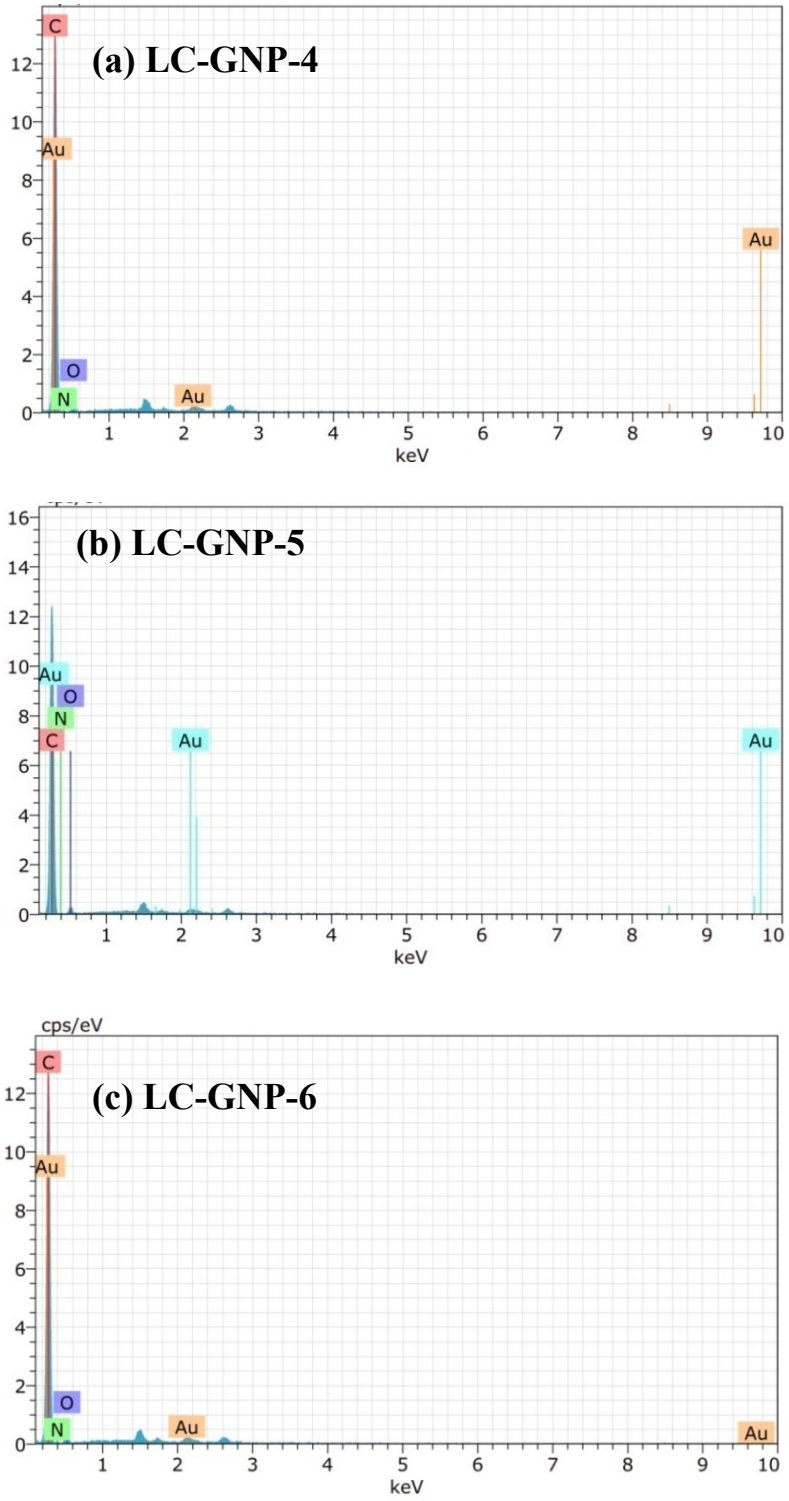

Figure S1. Profiles showing the energy-dispersive X-ray (EDX) spectroscopy elemental mapping images of **LC-GNP-4** (a), **LC-GNP-5** (b) and **LC-GNP-6** (c)**.** The profiles reveal the presence of carbon, nitrogen, oxygen and gold with carbon being the most abundant. The peak seen at ~ 2 keV in each profile especially implies the presence of GNPs.

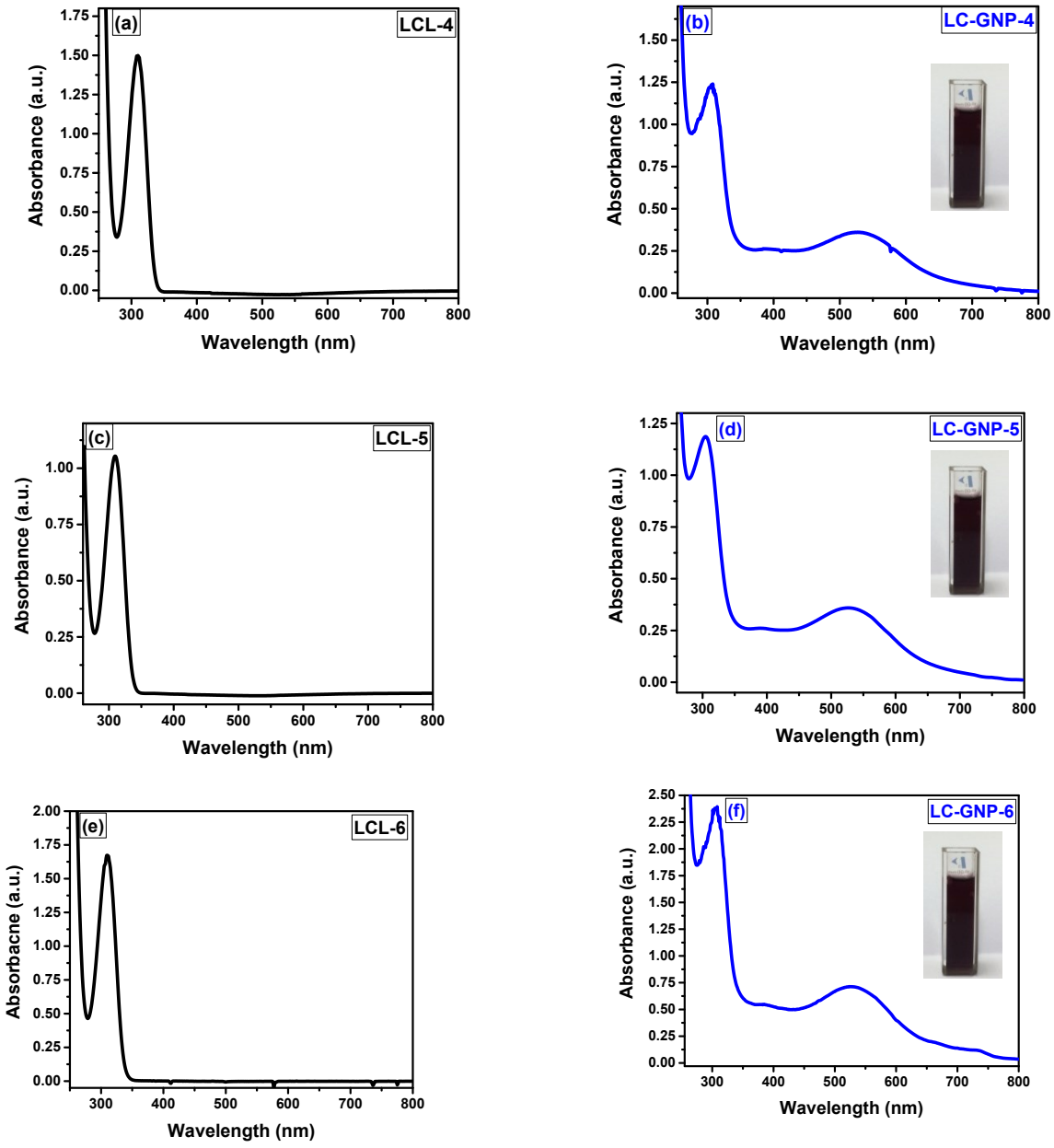

Figure S2. UV-Vis spectra of liquid crystalline ligands, **LCL-4** (a), **LCL-5** (c) & **LCL-6** (e) and liquid crystalline GNPs, **LC-GNP-4** (b), **LC-GNP-5** (d) & **LC-GNP-6** (f). Note that each spectrum of LC-GNPs shows a strong absorption peak at ~300 nm due to n-π* transition of organic segments as well as a broad band at ~530 nm due to SPR of GNPs. Inset of panels (b), (d) and (f) show the solutions of GNPs placed UV-Vis cuvettes.

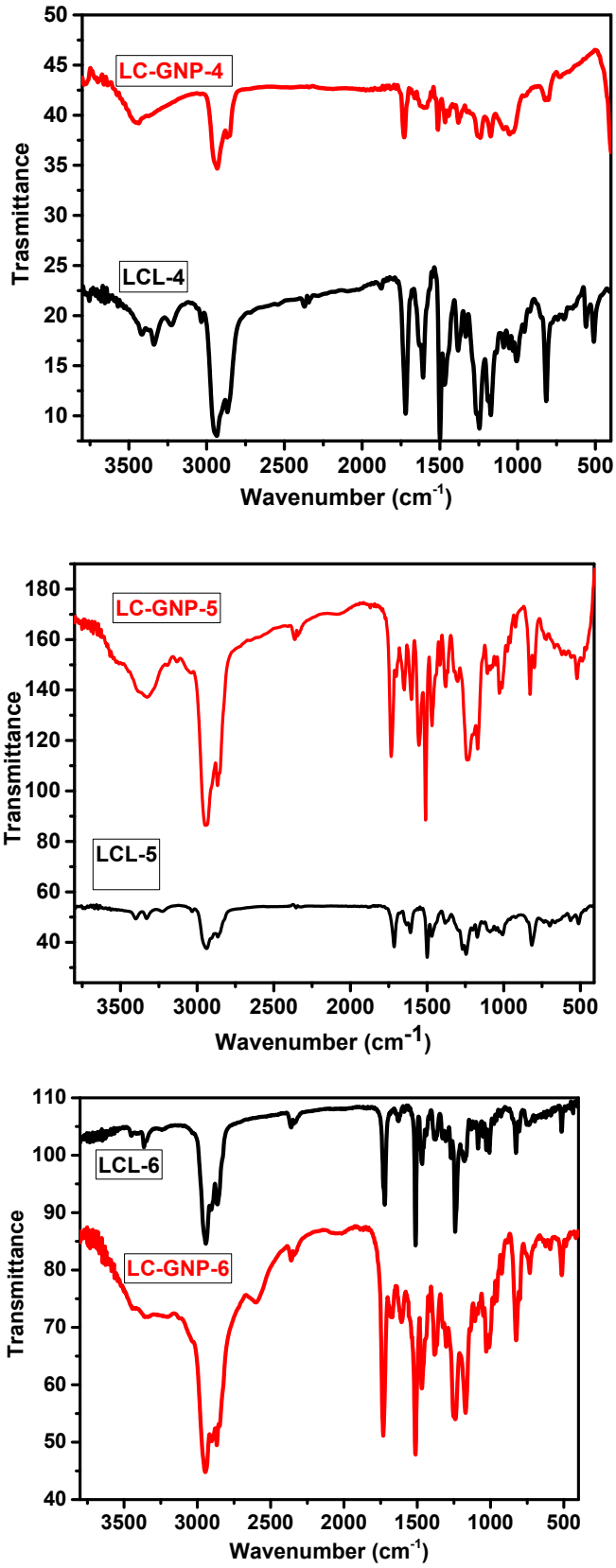

Figure S3: FTIR spectra of drop-coated film (over NaCl cell) of LCLs (black traces) and LC-GNPs (red traces).

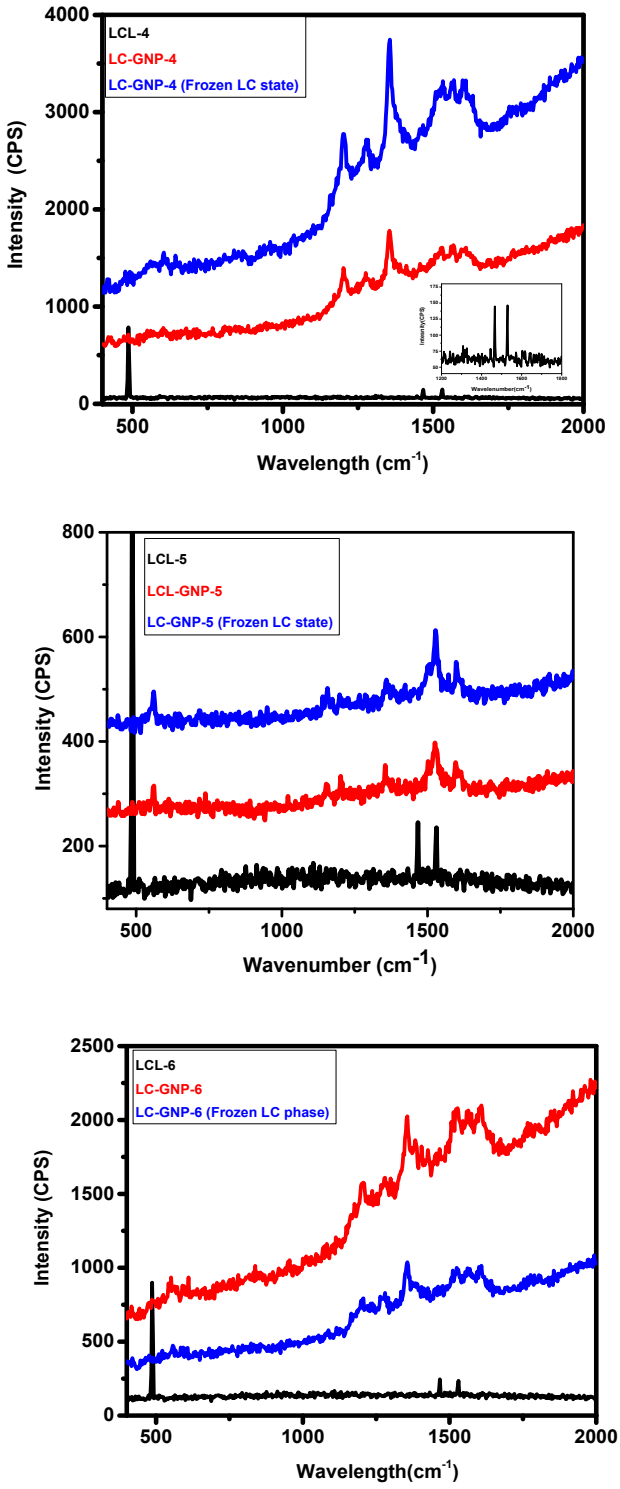

Figure S4. Raman spectra of **LCLs** (black traces), **LC-GNPs** (red-traces) and the frozen LC state of **LC-GNPs** (blue traces)**.**

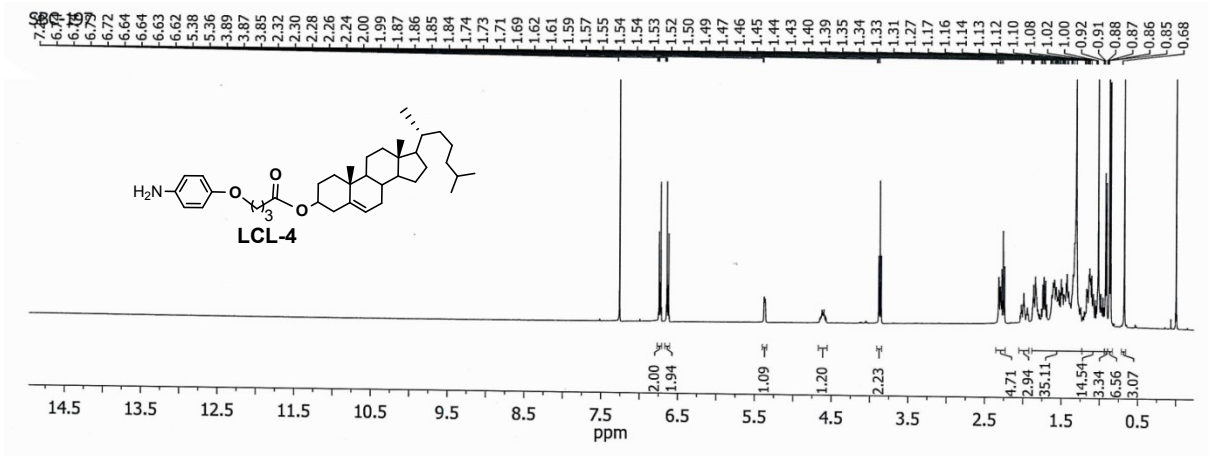

Figure S5. ^{1}H NMR spectrum of **LCL-4** (400 MHz; $CDCl_3$)

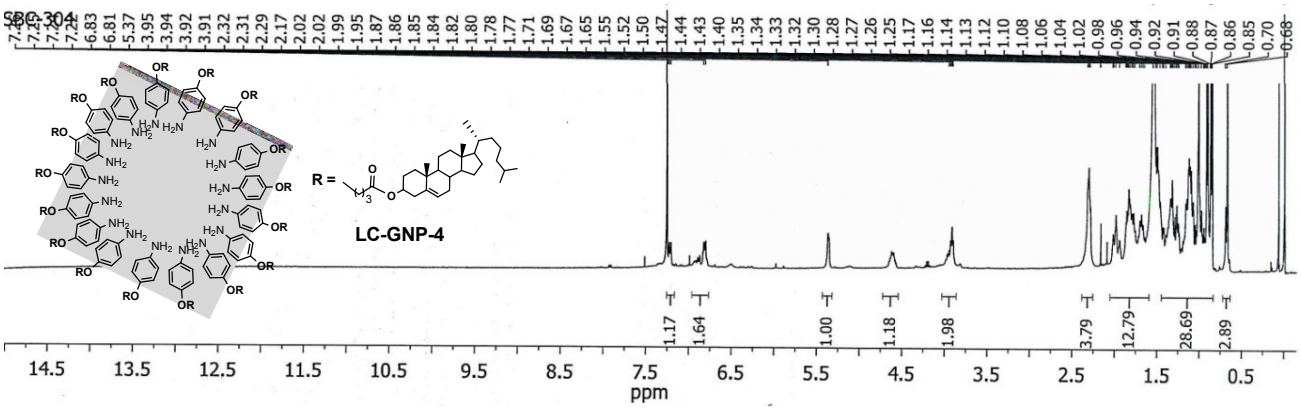

Figure S6. ^{1}H NMR spectrum of **LC-GNP-4** (400 MHz; $CDCl_3$) that was prepared by solution method

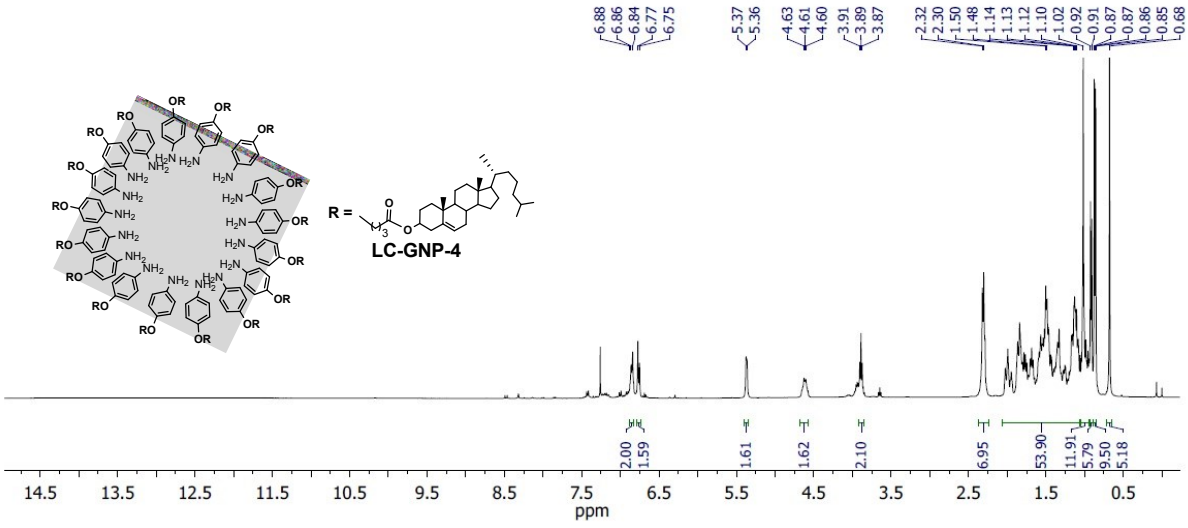

Figure S7. ^{1}H NMR spectrum of **LC-GNP-4** (400 MHz; $CDCl_3$) which was prepared by drop-coating method.

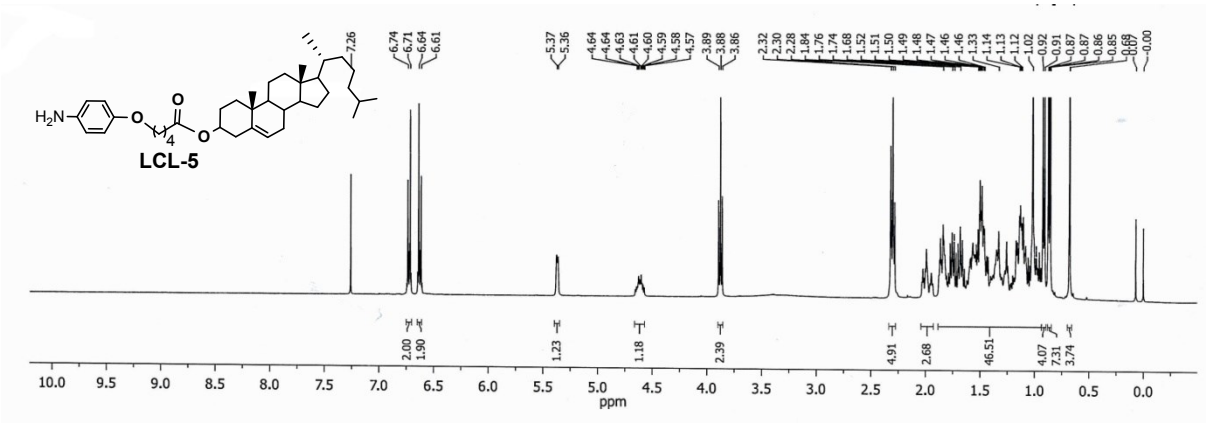

Figure S8. ^{1}H NMR spectrum of **LCL-5** (400 MHz; $CDCl_3$)

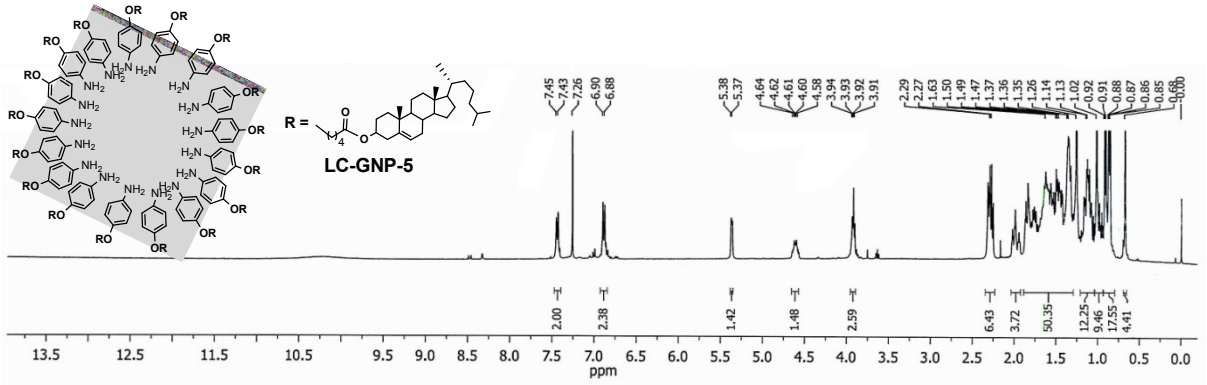

Figure S9. ^{1}H NMR spectrum of **LC-GNP-5** (400 MHz; $CDCl_3$) which was prepared by solution method

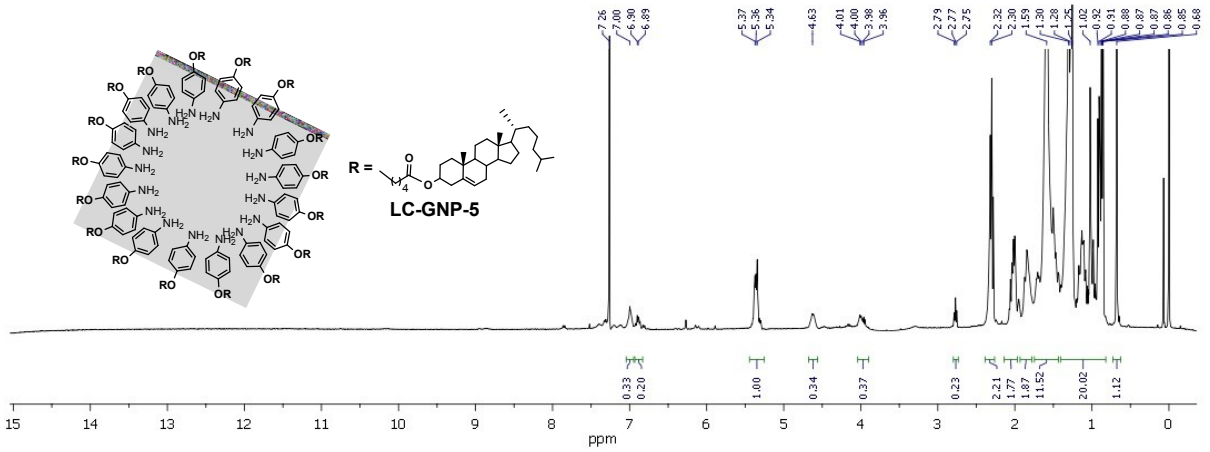

Figure S10. ^{1}H NMR spectrum of **LC-GNP-5** (400 MHz; $CDCl_3$) which was prepared by drop-casting method

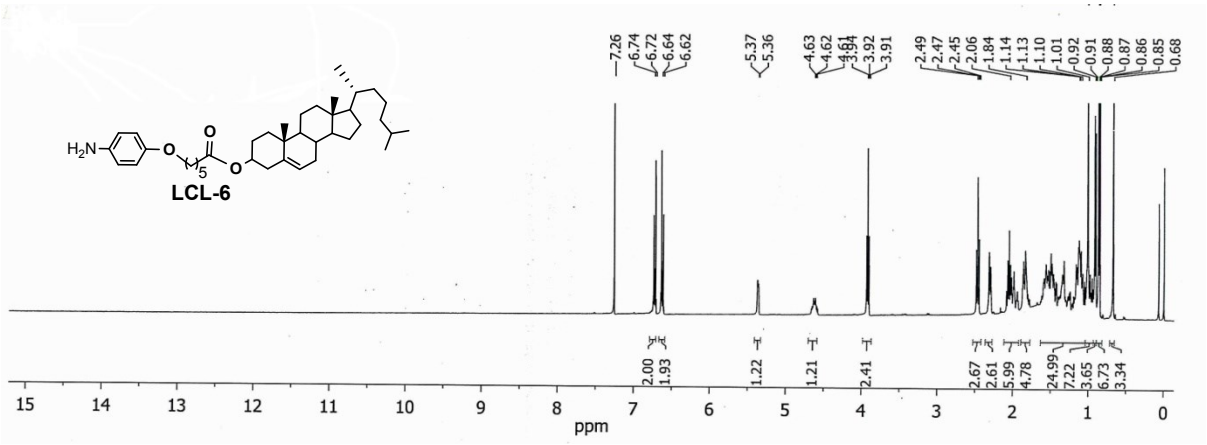

Figure S11. ^{1}H NMR spectrum of **LCL-6** (400 MHz; $CDCl_3$)

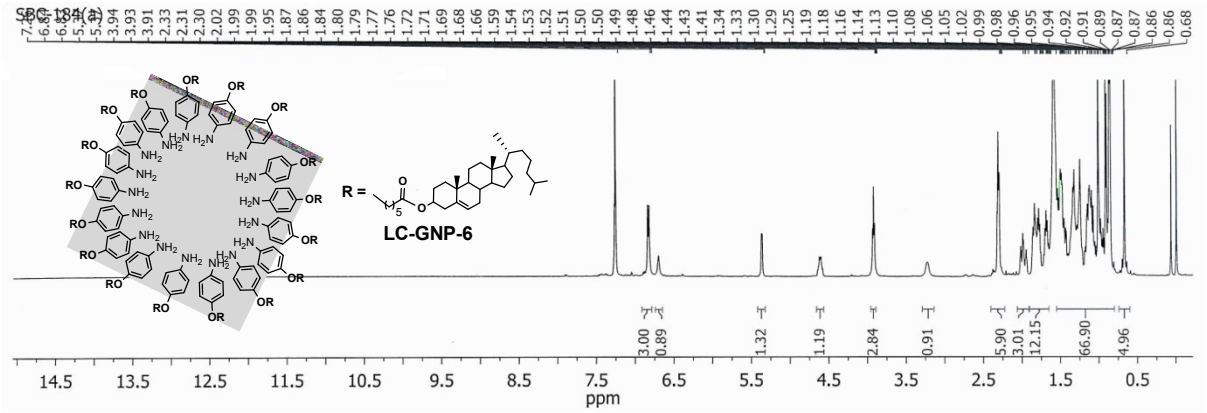

Figure S12. ^{1}H NMR spectrum of **LC-GNP-6** (400 MHz; $CDCl_3$) which was prepared by solution method

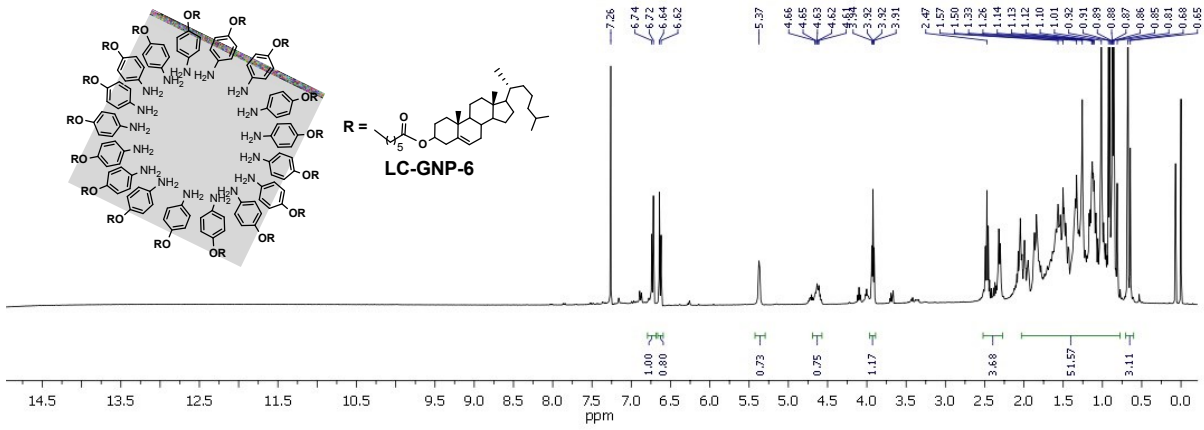

Figure S13: ^{1}H NMR spectrum of **LC-GNP-6** (400 MHz; $CDCl_3$) which was prepared by drop-casting method

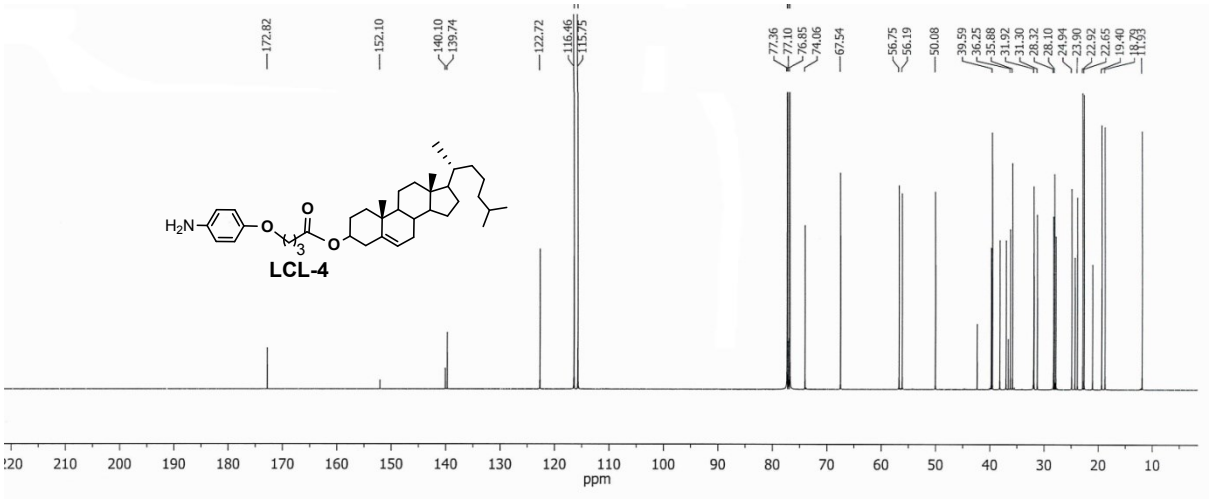

Figure S14.[13]C NMR spectrum of **LCL-4** (100 MHz; $CDCl_3$)

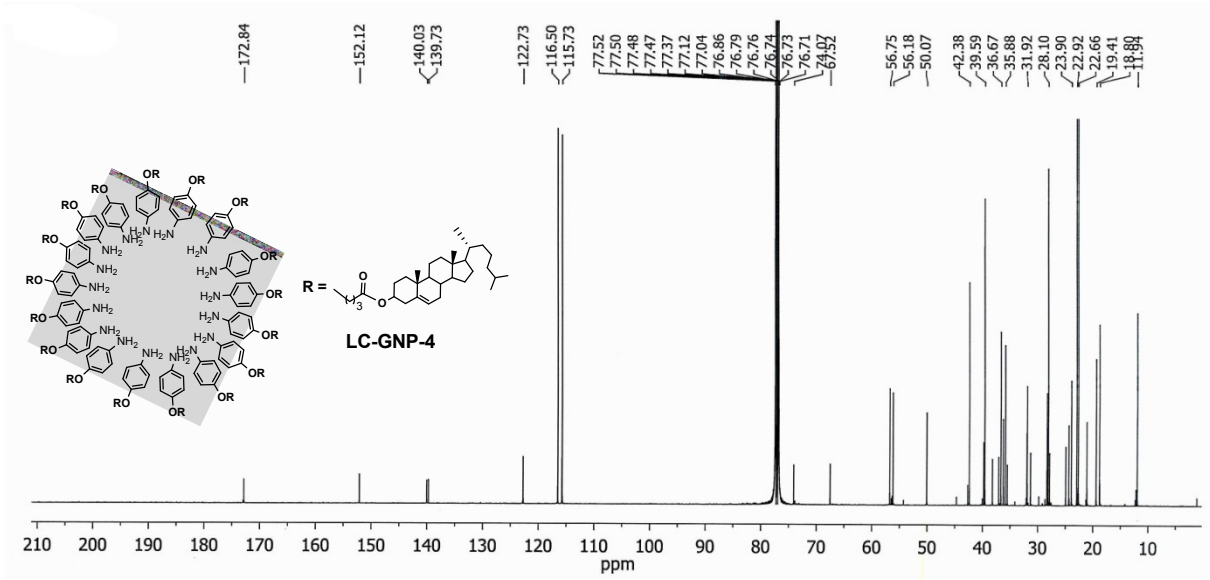

Figure S15.[13]C NMR spectrum of **LC-GNP-4** (100 MHz; $CDCl_3$)

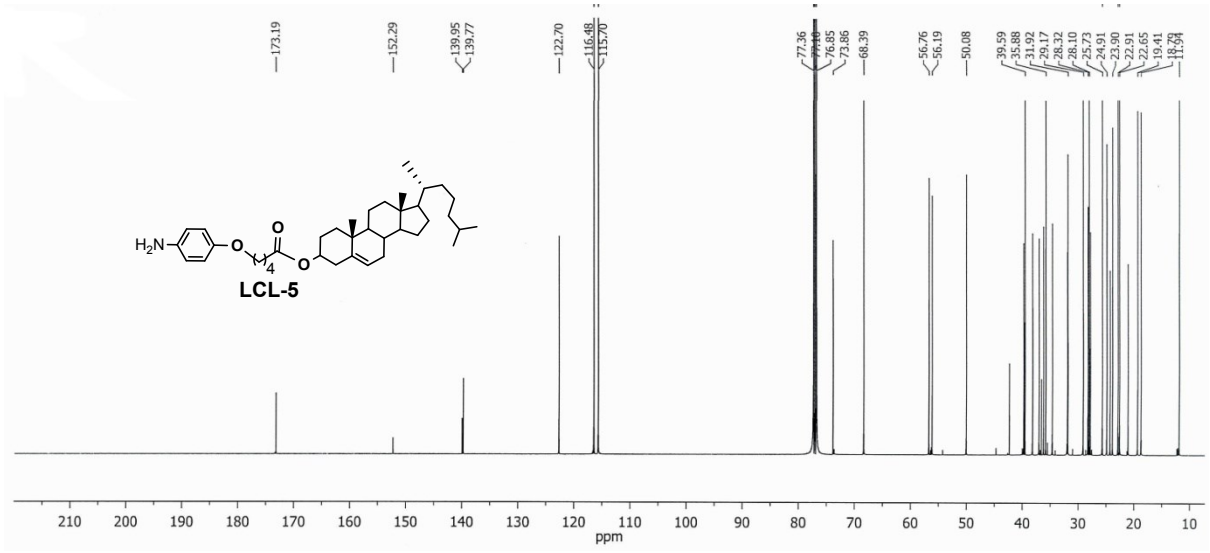

Figure S16.[13]C NMR spectrum of **LCL-5** (100 MHz; $CDCl_3$)

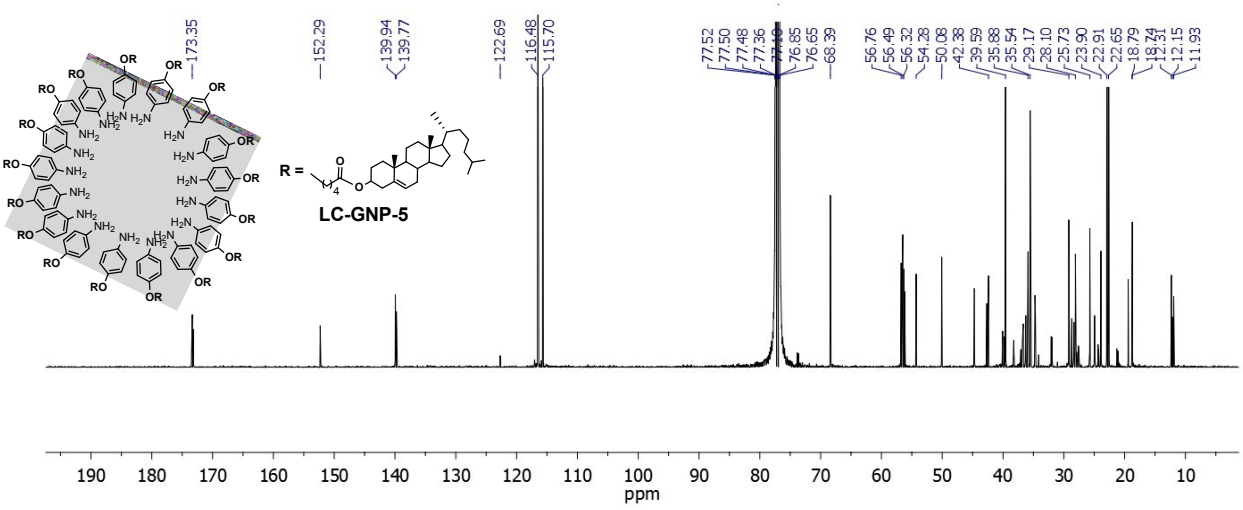

Figure S17.[13]C NMR spectrum of **LC-GNP-5** (100 MHz; $CDCl_3$)

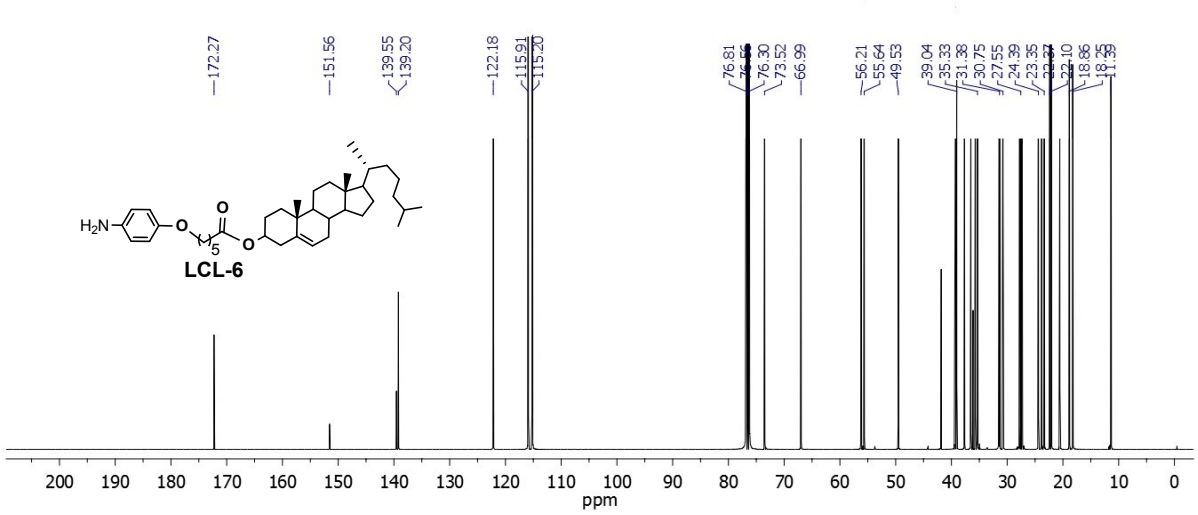

Figure S18.^{13}C NMR spectrum of **LCL-6** (100 MHz; $CDCl_3$)

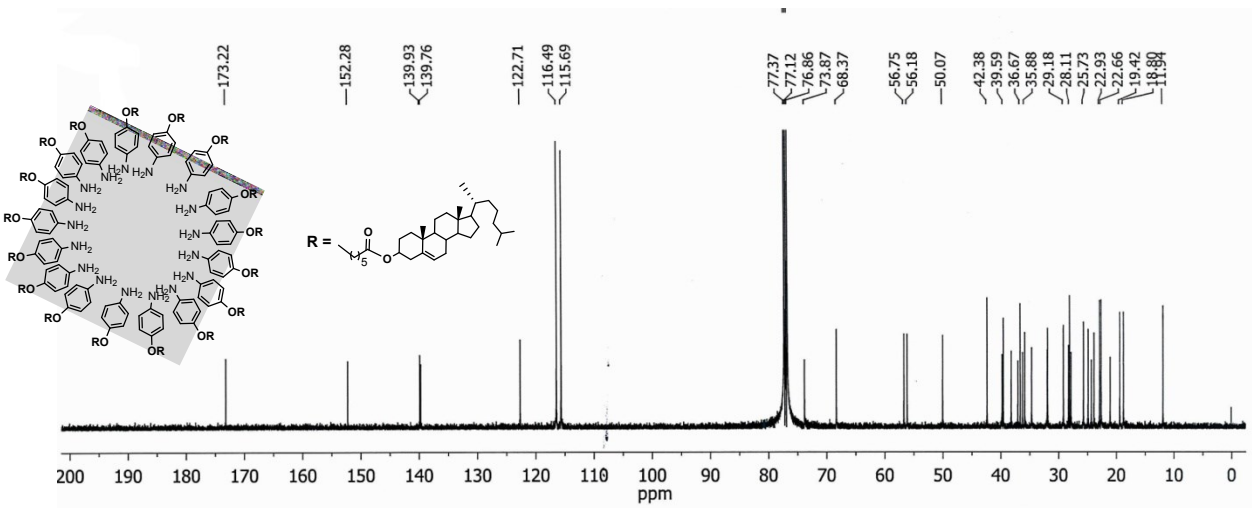

Figure S19.^{13}C NMR spectrum of **LC-GNP-6** (100 MHz; $CDCl_3$)

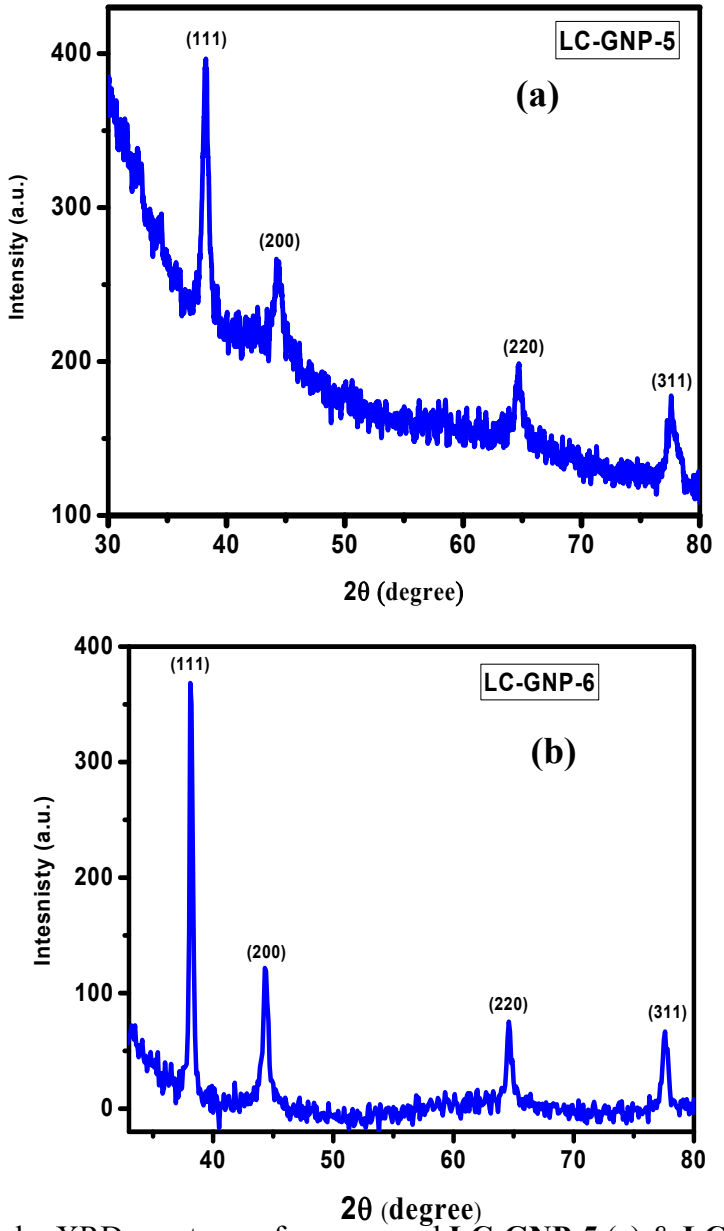

Figure S20: Powder XRD spectrum of as-prepared **LC-GNP-5** (a) & **LC-GNP-6** (b)

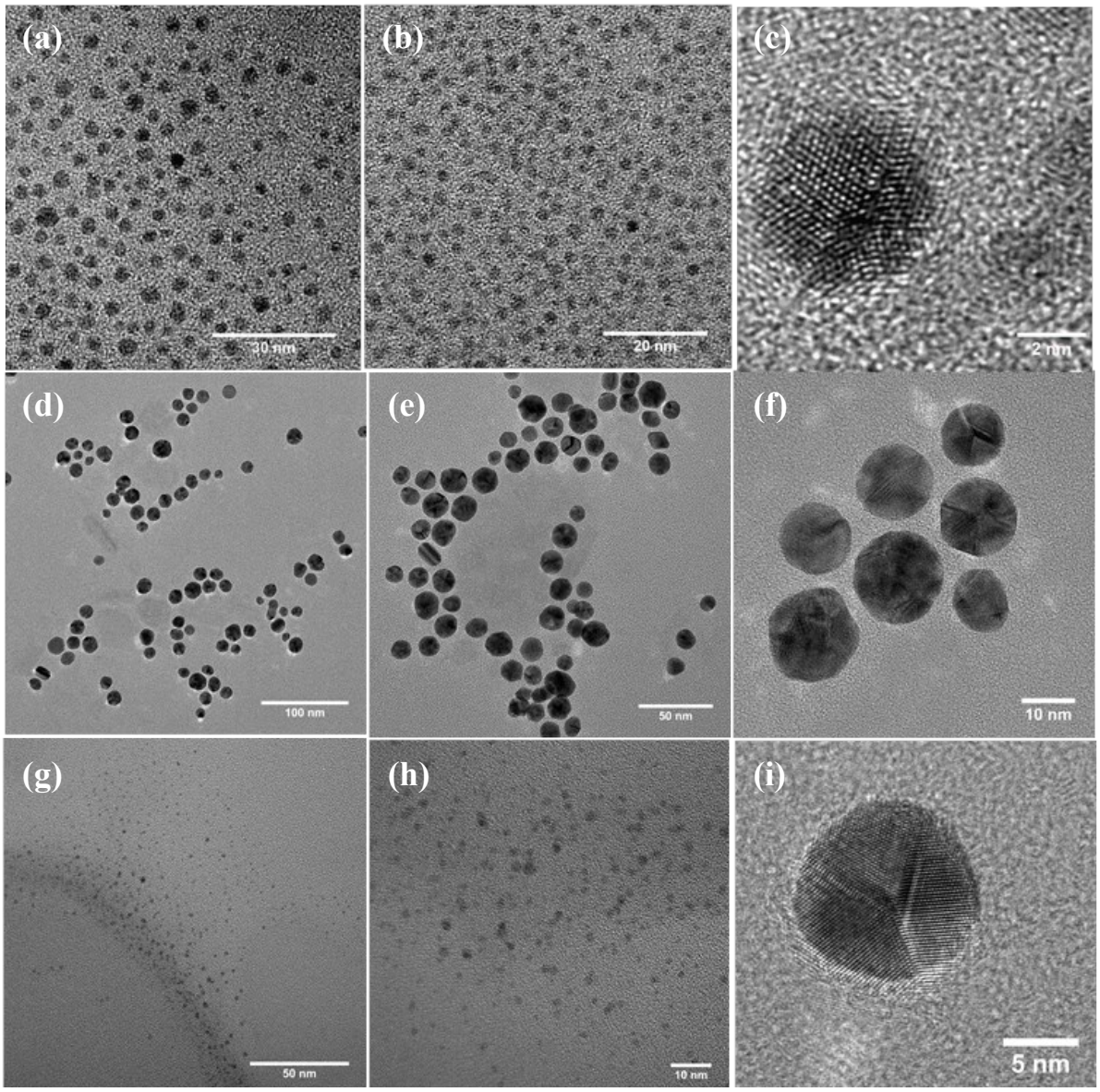

Figure S21: High-resolution TEM (HRTEM) images recorded at different scale bars for the sample (a), (b) & (c) **LC-GNP-4**, (d), (e) & (f) **LC-GNP-5** and (g), (h) & (i) **LC-GNP-6** drop casted on carbon coated copper grid. Although the images reveal the variations in shape and size, the spherically-shaped GNPs dominate.

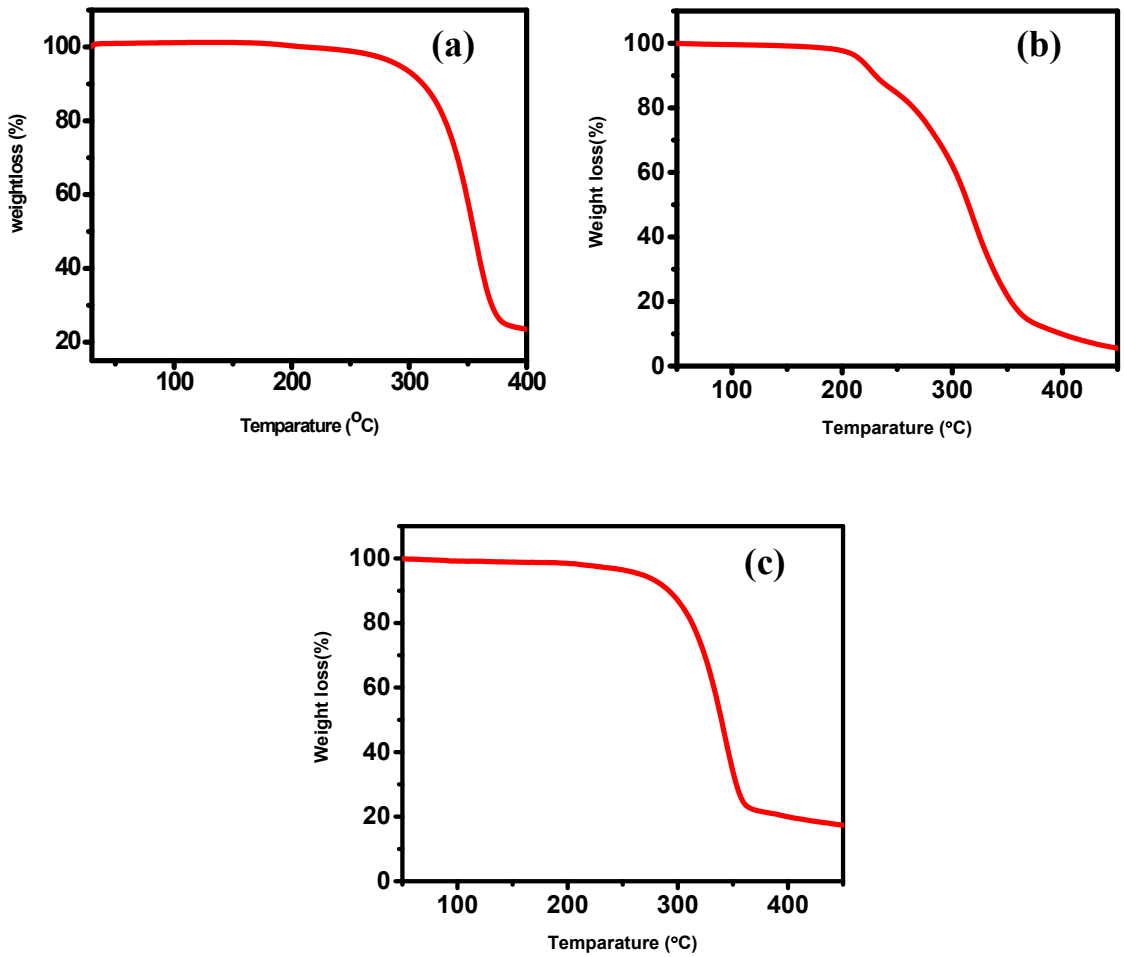

Figure S22: TGA traces of **LC-GNP-4** (a), **LC-GNP-5** (b) and **LC-GNP-6** (c). These traces indicate that the LC-GNPs are stable at least up to 200 °C.

Determination of particles and other parameters

S.No	GNPs	Particle Size	Total Au atoms	Surface Au atoms	No. of Ligands
1	**LC-GNP-4**	3.3 nm	982	395	85
2	**LC-GNP-5**	2.1 nm	257	156	35
3	**LC-GNP-6**	1.8 nm	162	115	26

- Average particle size (diameter) from TEM = **3.3nm**
- Radius = **1.65 nm**

Considering gold nanoparticle as spherical objects, i.e., Spherical Cluster Approximation (SCA)

Mean number of gold atoms per particle [1,2] : N (no of particles in a cluster) = $R_c^3 / R_a^3 = (1.65)^3/(0.166)^3 = 4.4921/ 0.004574 =$ **982 atoms/particle**

Number of particles on the surface of the spherical cluster[1,2] $N_s = 4N^{2/3} = 4 \times 982^{2/3} = 4 \times 98$ = **396 atoms**

Ligand coverage calculation

Number of ligands= Surface area of nanoparticle/surface area of amine on the gold

(The surface area of amine on the gold atom = 0.4 nm^2)

1) For **LC-GNP-4** the surface area of the nanoparticle is = $4\pi r^2 = 34.21$ nm^2

Hence the number of ligands = 34.21/0.4 = 85

2) For **LC-GNP-5** the surface area of the nanoparticle is = $4\pi r^2 = 13.85$ nm^2

Hence the number of ligands = 13.85/0.4 = 35

3) For **LC-GNP-6** the surface area of the nanoparticle is = $4\pi r^2 = 10.81$ nm^2

Hence the number of ligands = 10.81/0.4 = 26

References

1. R. L. Johnston, 'Atomic and Molecular Clusters', Taylor & Francis, **2002.**
2. D. J. Lewis, T. M. Day, J. V. Mac Pherson, Z. Pikramenou, *Chem. Commun*., **2006**, 1433.
3. A. Sharma, T. Mori, H.-C. Lee, M. Worden, E. Bidwell, T. Hegmann. *ACS Nano,* **2014**, 8, 12, 11966–11976

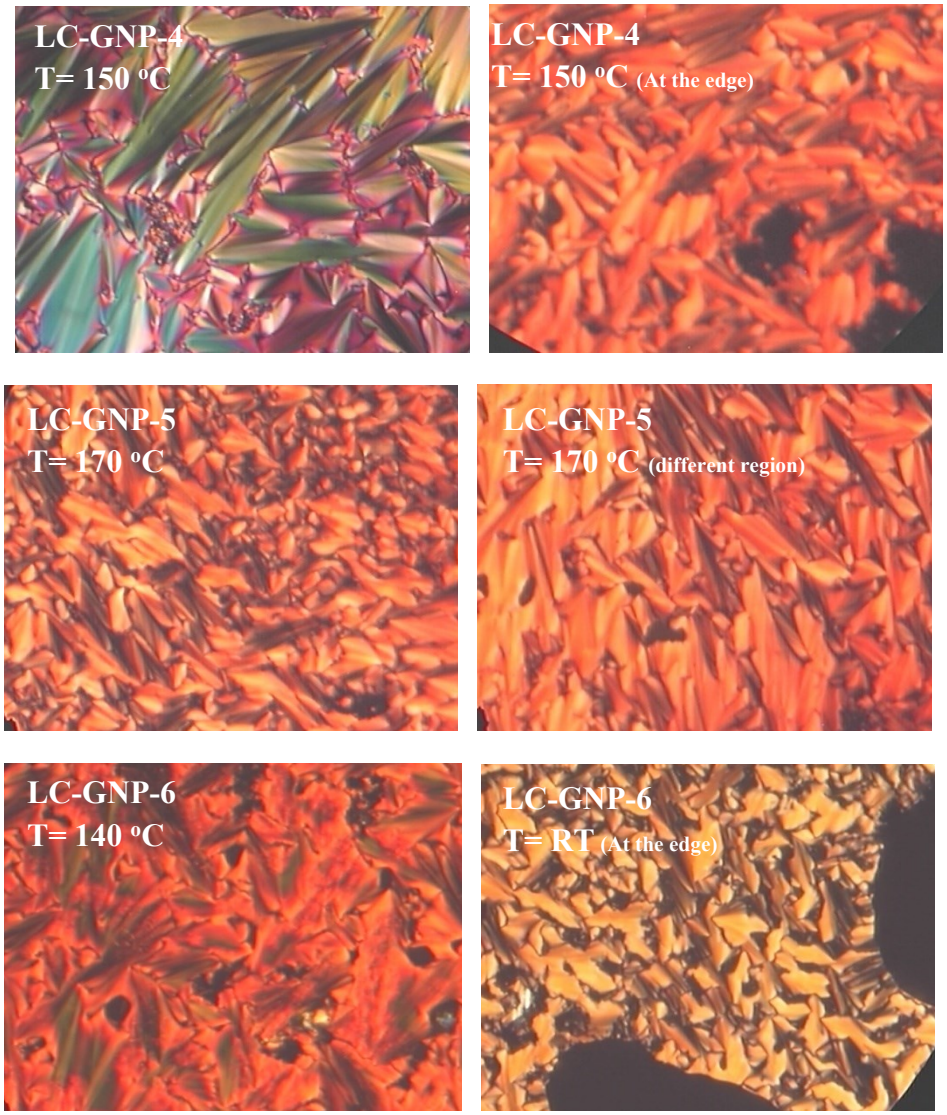

Figure S23: Optical photomicrographs of the textures observed for the LmX* of **LC-GNPs** under a polarizing microscope

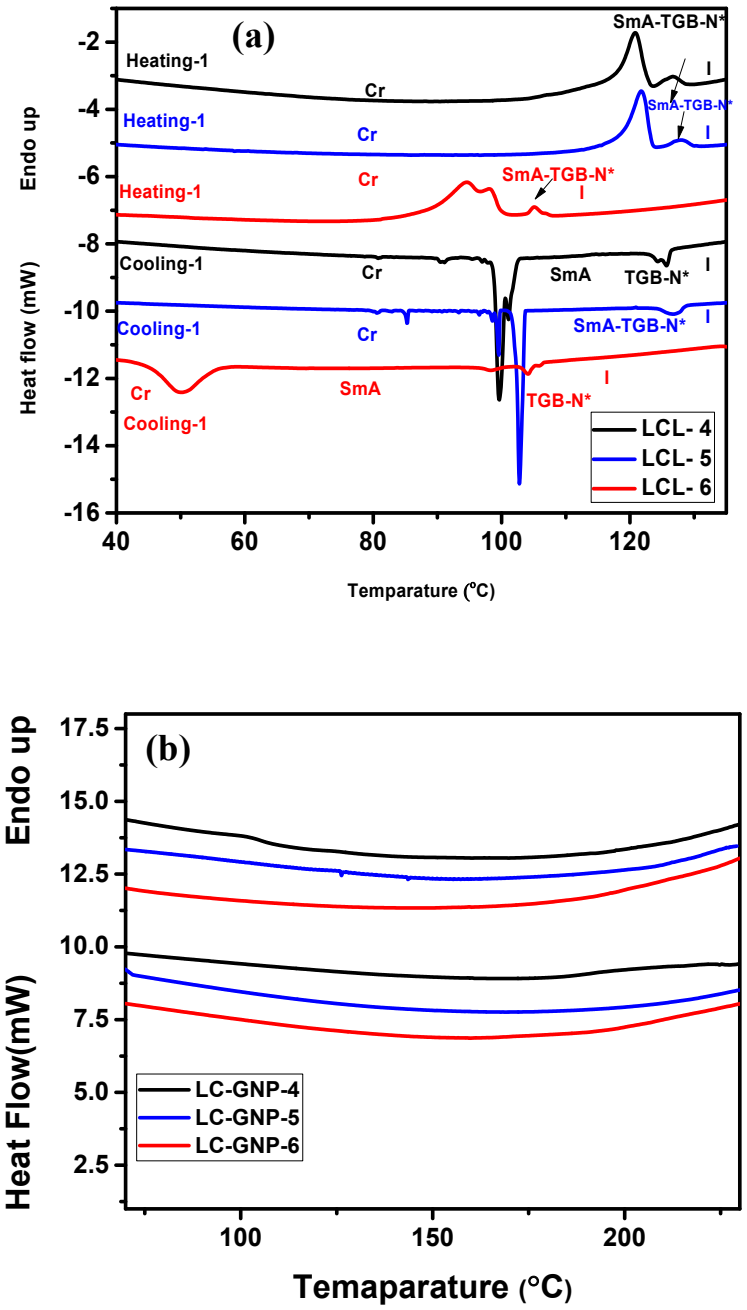

Figure S24: DSC thermograms registered during the first heating-cooling cycles of the dimer-like ligands (LCLs) (a) and LC-GNPs (b)

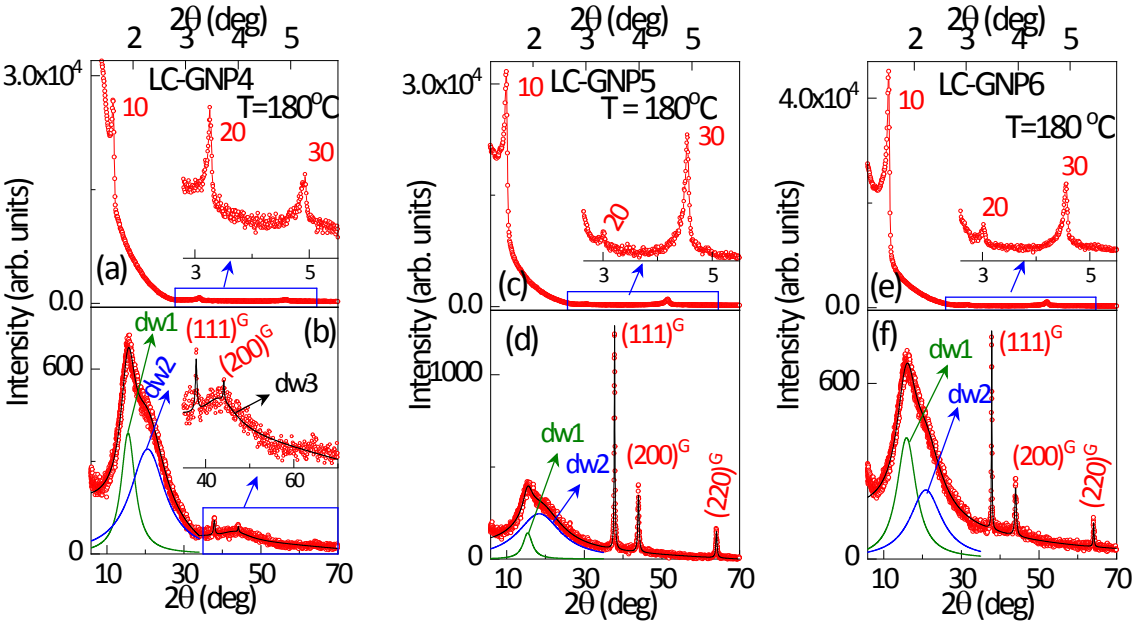

Figure S25: X-ray diffraction profiles in the low angle (a,c,e,) and wide angle (b,d,f) regions obtained for (a) **LC-GNP4** (at 180°C), (b) **LC-GNP5** (at 180°C) and (c) **LC-GNP6** (at 180°C) samples in the LmX* phase. The sharp reflections seen in the low angle region corresponds to the lamellar ordering, and in the wide angle region they arise from the FCC lattice of Au(0); for purposes of better view the harmonics due to lamellar ordering are shown on an enlarged scale in the insets of panels (a,c,e). The diffuse peaks dw1 and dw2, becoming more prominent after the deconvolution procedure represent the intermolecular ordering within the lamellae and show up as two reflections owing to different spatial ordering of the cholesterol group and the hydrocarbon linkers. The diffuse peak dw3 arising due to disordering of the gold atoms, being most prominent in **LC-GNP4**, is shown as an inset in panel (b). The fitting of the overall data (in panels (b), (d) and (f)) comprising multiple peak functions, is shown as a dark line.

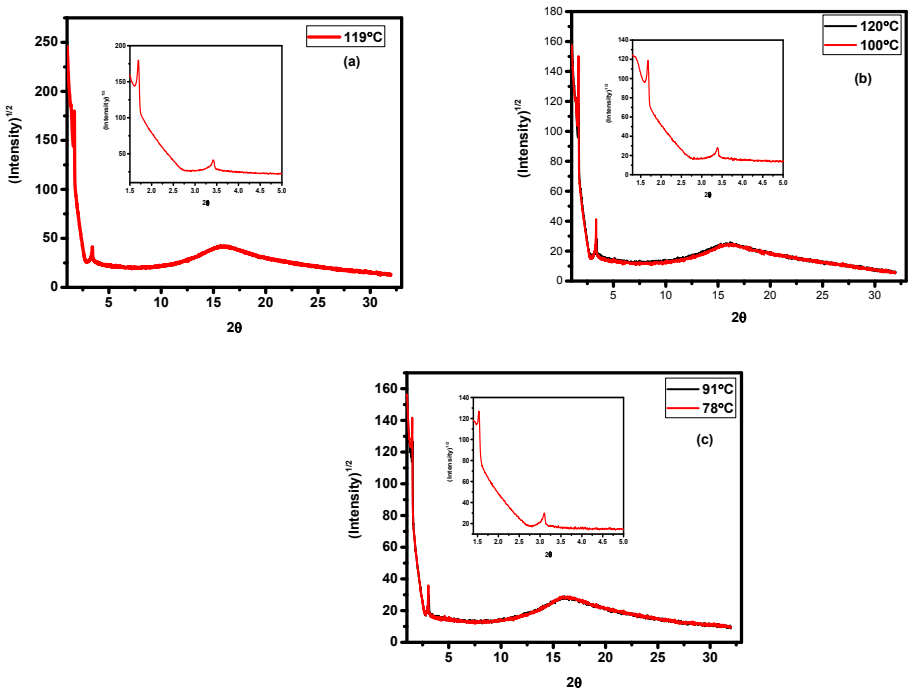

Figure S26: The 1D intensity vs. 2θ profiles obtained for the SmA phase of (a) **LCL-4,** (b) **LCL-5** and (c) **LCL-6** as a function of temperature. Note that each trace comprises three sharp reflections (inset) in the low-angle region and two diffuse peaks arising at the wide angle ragion respectively due to lamellar structure, liquid-like arrangement of the mesogens within the layers.

Table S1: XRD data of the SmA phase of ligands **LCL-4**, **LCL-5** and **LCL-6**. The spacing (*d*) corresponding to the low-angle reflections and the wide-angle peak positions are given.

LCL [Calculated mol. Length, *L* (Å)]	Temperature (°C)	Layer spacing – *d*; low-angle peak positions (Å) Peaks arising due to layered structure			Wide-angle peak positions (Å)	d_1 / *L*
		d_1	d_2	d_3	Peaks due to fluid nature of the phase	
LCL-4 (28.1)	119 °C	52.00	25.82	-	5.58 4.50	1.85
LCL- 5 (29.9)	120 °C	52.57	26.05	-	5.57 4.54	1.75
	100 °C	53.32	26.39	17.59	5.55 4.51	1.78
LCL- 6 (30.9)	91°C	57.66	28.48	-	5.49 4.49	1.86
	78 °C	58.34	28.89	19.25	5.48 4.58	1.88

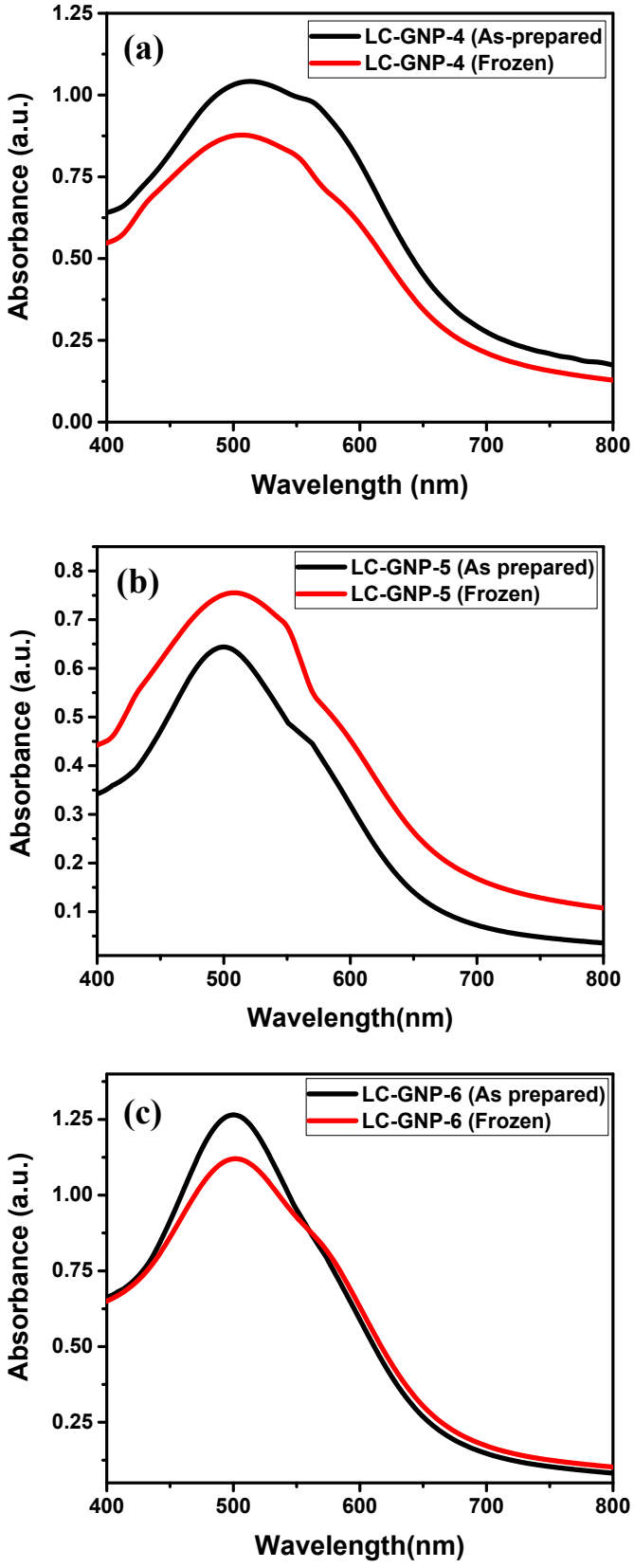

Figure S27: UV-Vis spectra of the thin-films of frozen LC phase (red-traces) and that of as-prepared (drop-casted) samples: (a) **LC-GNP-4**; (b) **LC-GNP-5** and **LC-GNP-6**

Table S2: Spacings, *d*, (in Å) associated with the lamellar ordering and spatial correlation of the gold atoms at three different temperatures for the studied materials. *L*= Calculated end-to-end molecular length (in Å)

LC-GNP-6 (*L*=94.8)	RT	T = 80 °C	T = 180 °C
d_1	61.27	61.54	58.67
d_2	30.48	30.51	29.34
d_3	20.19	20.29	19.40
diffuse (*dw*1)	5.42	5.52	5.58
diffuse (*dw*2)	4.30	4.38	4.26
Au-peak1	2.37		2.38
Au-peak2	2.05		2.06
Au-peak3	1.45		1.45
LC-GNP-5 (*L*= 92.8)	RT	T = 110 °C	T = 180 °C
d_1	58.73	59.52	59.09
d_2	19.42	19.63	29.38
d_3			19.48
diffuse (*dw*1)	5.48	5.57	5.74
diffuse (*dw*2)	4.41	4.32	4.81
Au-peak1	2.37		2.38
Au-peak2	2.06		2.06
Au-peak3	1.45		1.45
LC-GNP-5 (*L* = 89.2)	RT	T = 110 °C	T = 180 °C
d_1	55.44	55.09	54.57
d_2	27.62	27.46	27.10
d_3	18.32	18.28	18.04
diffuse (*dw*1)	5.48	5.58	5.71
diffuse (*dw*2)	4.28	4.29	4.31
Au-peak1	2.37		2.37
Au-peak2			2.05
Au-peak3			
Au-peak (dw3)	2.03		2.09

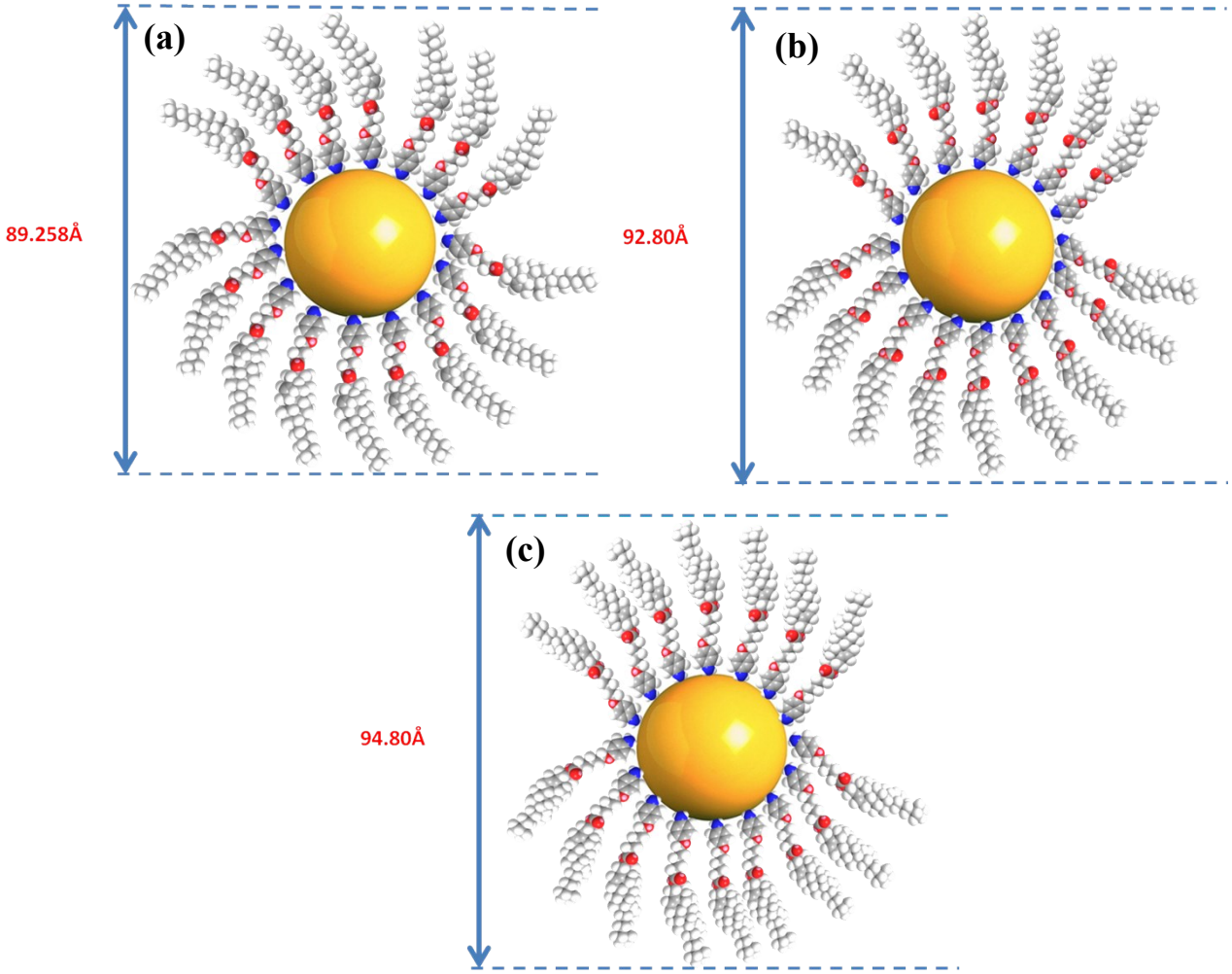

Figure S28: Schematic representation of **LC-GNP-4** (a), **LC-GNP-5** (b) and **LC-GNP-5** (c) covered with monolayer of respective ligands **LCL-4**, **LCL-5** and **LCL-6**. The end-to-end GNP lengths are also shown.

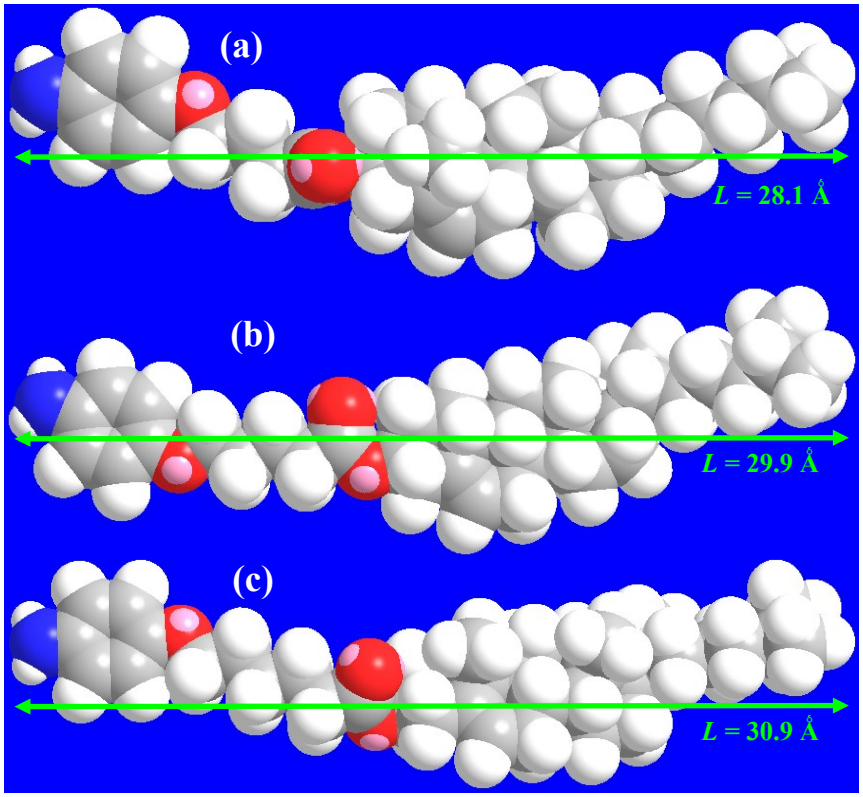

Figure S29: Energy-minimized ball-and-stick models (derived from MM2 calculation of ChemBioDraw Ultra 12.0) of the most extended form (all-*trans* conformation) of ligands (a) **LCL-4**, (b) **LCL-5** and (c) **LCL-6**.

Table S3. CD spectroscopic data obtained for the LmX* phase of LC-GNPs

LC-GNPs	LmX* Phase Temperature (°C)	CD	
		λ_{max} (nm)	CD (mdeg)
LC-GNP-4	200	634.5, 377.0	79.96, -118.29
	190	635.0, 384.5	85.25, -125.04
	180	631.0, 378.5	91.0, -122.13
	170	633.0, 387.5	114.5, -130.80
	160	632.0, 386.0	169.5, -146.70
	150	624.1, 384.0	196.3, -157.60
	RT (25)	623.0, 381.0	197.3, 158.01
LC-GNP-5	200	517.5, 365.5	-1.88, -21.52
	190	516.5, 370.5	-1.39, -25.07
	180	527.0, 370.0	-1.86, -29.63
	170	526.0, 369.5	-0.60, -41.85
	160	530.5, 368.0	1.79, -44.92
	150	541.0, 372.5	3.12, -47.01
	RT (25)	531.5, 370.5	2.66, -46.44
LC-GNP-6	200	526.5, 355.0	0.003, -0.30
	190	525.0, 363.0	1.85, -10.66
	180	533.0, 359.0	7.35, -22.28
	170	531.0, 355.5	23.46, -42.11
	160	526.0, 351.5, 272.5	36.41, -66.05, -20.55
	150	534.5, 347.5, 270.5	43.98, -86.34, -41.31
	140	541.0, 345.5, 251.0	36.40, -96.96, 106.45
	130	539.0, 343.5, 257.0	42.82, -89.59, -105.71
	RT (25)	552.5, 341.0, 254.0	36.19, -95.80, -106.05

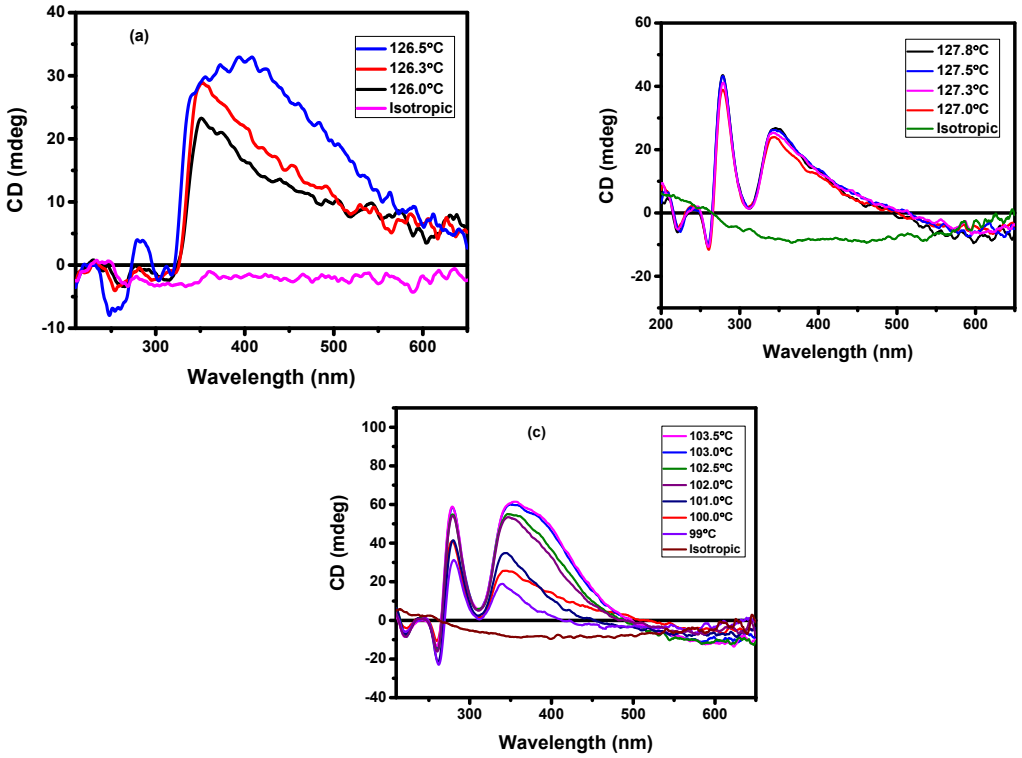

Figure S30: CD spectra of amines (a) **LCL-4** (b) **LCL-5** and (c) **LCL-6** recorded as a function of temperature in the N* phase.

Table S4. CD spectroscopic data obtained for the N* phase of LCLs.

Compounds	Chiral LC phase	Temperature (°C)	CD	
			λ_{max} (nm)	CD (mdeg)
LCL-4	N*	Isotropic	---	---
		126.5	392.3	32.9
		126.3	350.8	29.0
		126.0	350.7	23.3
LCL-5	N*	Isotropic	---	---
		127.8	345.1, 278.4	26.7, 43.5
		127.5	343.7, 278.3	26.7, 43.6
		127.3	343.8, 279.3	24.7, 41.1
		127.0	342.8, 278.9	23.9, 38.9
LCL-6	N*	Isotropic	---	---
		103.5	355.4, 277.9	61.4, 58.7
		103.0	358.0, 277.8	59.7, 58.6
		102.5	347.5, 278.8	55.0, 54.8
		102.5	347.4, 279.2	53.5, 54.1
		101.0	343.5, 279.7	34.8, 40.7
		100.0	341.5, 279.6	25.6, 40.7
		99.0	339.6, 280.1	18.9, 31.2

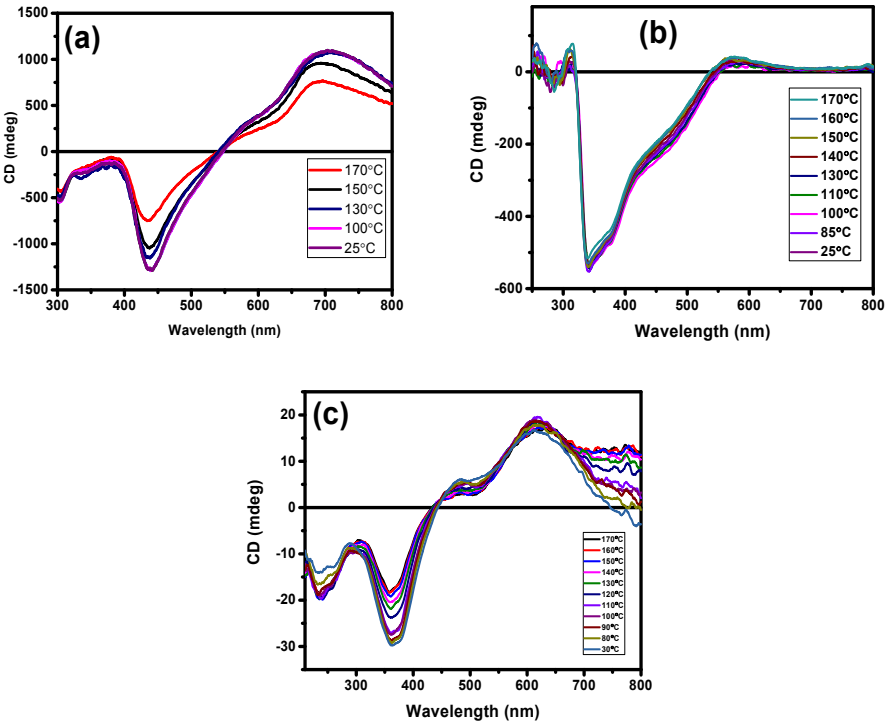

Figure S31: CD spectra of the LmX* phase of the **LC-GNP**s placed between two quartz slides treated for homeotropic orientation: **LC-GNP-4** (a), **LC-GNP-5** (b) & **LC-GNP-6** (c)

Elimination of linear dichroism (LD) and linear birefringence (LB) artefacts

Linear dichroism and linear birefringence are absorptive and dispersive phenomena respectively and are related to one another by Kramers-Kronig relations[1]. These photoselectively induced linear artefacts (PSLA) exists before the molecular rotation[1]. These artefacts change the shape of the signals upon rotating the sample film about the optic axis of the incoming light [2-4]. This observation has been mathematically modelled to find out the effect of LD on the circular dichroism (CD) signal which is given by the following expressions.

$$\delta_{app} = \delta_{real} - 0.298\ p\ Cos\ 2\alpha$$

Here, δ_{app} - Observed CD value

δ_{real} - Real CD value

p - Linear dichroism

From further calculations it can be seen that the value of δ_{real} is independent of angle α where as p is dependent on it. Hence upon rotation, the value which gets affected will be LD and LB but not CD. Thus the artefacts such as LD and LB can be eliminated by rotating the sample normal to the beam direction and recording the spectra and obtaining δ_{real} value [1-4]. LD is absent in the system i.e p = 0 irrespective of rotation $\delta_{real} = \delta_{app.}$

References

1) S. C. Bjiirling, R. A. Coldbeck, S. J. Milder, C. E. Randall, J. W. Lewis and D. S. Kliger, *The Journal of Physical Chemistry*, 1991, 95, 12, 4685 - 4694

2) M.B. Jane, T, Schneider and I. F. Maestre, *J. Mol. Biol*., 1970, 52, 521-541

3) T. Narushima and H. Okamoto*, Scientific Reports*, 2016, 6, 35731

4) J. H. Freudenthal, E. Hollis, B. Kahr, *Chirality*., 2009, 21, E20-27

Preparation Quartz Plates (cell) treated for homeotropic orientation

As discussed above, the linear birefringence (LB) can also produce a CD signal. To eliminate this error, CD measurements of the LmX* phase, as a function of temperature, were undertaken using quartz plates treated for mesogens' homeotropic orientations. That is, the usage of quartz plates treated for homeotropic anchoring reduces or eliminates the effect of birefringence significantly. Silane treated quart plates ensured homeotropic alignment. The quartz plates were initially washed with water and sonicated for 10 mins. They were then washed with HPLC grade acetone and air-dried. The 0.1 % solution of triethoxy silane in water was prepared, and the quartz plates were dipped for about 1 min. After air-drying, the plates were heated at 150 ^{o}C for 3 hrs, Our study shows that the LmX* phase's CD activity more or less remains the same whether the substrate (cell) fabricated were just quartz plates or treated with a silane solution for homeotropic alignment.